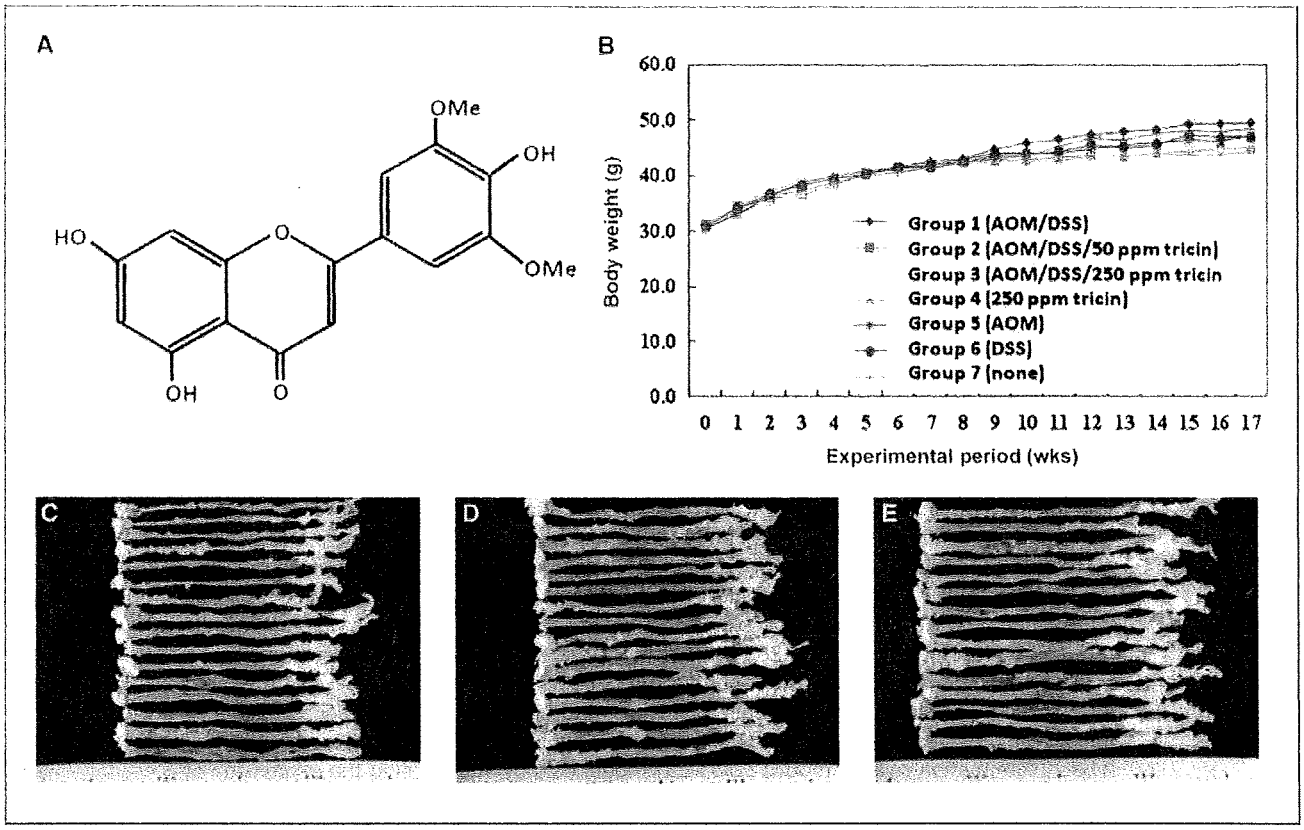

Fig. 1. *A*, the structure of tricin; molecular weight, 330.074. *B*, body weight changes of mice in all groups during the study. Dietary tricin (groups 2, 3, and 5) did not significantly affect the body weight gain. Macroscopic views of the colons from the mice of groups 1 (*C*), 2 (*D*), and 3 (*E*), which received AOM/DSS, AOM/DSS/50 ppm tricin, and AOM/DSS/250 ppm tricin, respectively, at the end of the study (week 18). Although a number of colonic tumors were observed in the mice of group 1, the numbers of the tumors found in groups 2 and 3 were smaller than that in group 1.

include antioxidative (13, 14), antiinflammatory, antiviral (15), and antihistamic (16) activities. These same biological activities have been observed in other promising cancer chemopreventive agents (17–20). The effects of tricin on oncogenesis have been investigated by Gescher et al. Their studies have shown that tricin suppresses the growth of human malignant breast tumor in nude mice (21). Dr. Gescher's group also reported that treatment with tricin-containing extracts from brown rice inhibit the proliferation of human colon and breast cancer cells *in vitro* (22). There are few reports on the effects of dietary tricin on intestinal carcinogenesis. Cai et al. (23) reported that feeding a diet containing 0.2% tricin decreased the size and the number of intestinal adenoma formed in $Apc^{Min/+}$ mice through the inhibition of cyclooxygenase (COX)-2 (23, 24). Dietary tricin did not affect tumor formation in the large bowel (23). Because the concentration of tricin in the mouse intestine is greater than the concentration in the plasma or liver when mice are fed diets containing tricin (25–28), we hypothesized that dietary tricin may affect and possibly inhibit chemically-induced colon carcinogenesis in rodents.

The current study was designed to explore the possible cancer chemopreventive efficacy of tricin. We investigated the effects of dietary tricin on large bowel oncogenesis using an azoxymethane (AOM)/dextran sodium sulfate (DSS)–treated mouse model, which is a useful animal model to study chemoprevention in inflammation-related colon carcinogenesis (29–34). The effects of dietary tricin on the expression of inflammatory enzymes, such as COX-2 (35–37) and inducible nitric oxide synthase (iNOS; refs. 37, 38), and inflammatory cytokines, such as tumor necrosis factor (TNF)-α, (39, 40) NF-κB (17, 40), inhibitor κB (IκB)α, and IκB kinase (IKK)β in the nonlesional colonic mucosa were examined to understand the mechanism(s) by which the compound modify AOM/DSS-induced colon carcinogenesis. In addition, we determined whether dietary tricin affects the chromosomal instability (41) of adenocarcinoma cells by counting the number of anaphase-bridging formations.

Materials and Methods

Chemicals

Tricin (>99% pure confirmed by high performance liquid chromatography) was isolated and prepared from the leaves of *Sasa albo-marginata* (Hououdou Co. Ltd.) by one (M.K.) of the authors (15). In brief, the dried leaves (50 kg) were combined with water (1,000 l) and extracted at 170°C over a period of 3 h. The extracted solution was filtered. The hot water extract of *Sasa albo-marginata* was fractionated successively with ethyl acetate and *n*-butanol. The ethyl acetate fraction (52.0 g) was fractionated using a silica gel 60 (Cica-reagent, 40-50 μm) column (inner diameter 6 × 50 cm, 500 g) and washed with *n*-hexane-ethyl acetate and methanol. This process yielded seven fractions (A-G). Chloroform was added to fraction F (1.50 g) to obtain a chloroform-soluble fraction and an insoluble fraction (solid phase). Tricin (10.0 mg) was recrystallized from the chloroform-soluble fraction as yellow,

needle-shaped crystals. Finally, a total of 8 g of tricin was prepared from 40,000 kg of the leaves and was used in this study.

AOM was purchased from Sigma-Aldrich. DSS with a molecular weight of 36,000 to 50,000 was obtained from MP Biomedicals, LLC. DSS 1.5% (*w/v*) was prepared shortly before use to induce colitis.

Animals and diets

Five-week-old male Crj: CD-1 (ICR) mice were purchased from Charles River Laboratories, Inc. All animals were housed in plastic cages (three or four mice/cage) and had free access to tap water and a basal diet, Charles River Formula-1 (Oriental Yeast, Co., Ltd.). The animals were kept in an experimental animal room under controlled conditions of humidity (50 ± 10%), light (12/12-h light/dark cycle) and temperature (23 ± 2°C). After 1 wk of quarantine, animals were divided into six experimental groups and one control group. Experimental diets were prepared by mixing tricin in powdered basal diet at two dose levels, 50 and 250 ppm. The highest dose was one eighth of the dose used by Cai et al. (23) because we investigated the potential clinical application of low doses of tricin.

Animal experiment

The experimental and study design were approved by the Committee of Kanazawa Medical University Animal Facility under the Institutional Animal Care guideline. All handling and procedures were carried out in accordance with the appropriate Institutional Animal Care Guidelines.

A total of 95 male ICR mice were divided into six experimental groups and one control group. Mice in groups 1 (n = 20), 2 (n = 20), and 3 (n = 19) were given a single i.p. injection of AOM (10 mg/kg body weight). Beginning 7 d after the AOM injection, they also received 1.5% (*w/v*) DSS in drinking water for 7 d. Beginning 1 wk following the final DSS exposure, the mice in groups 2 were fed an experimental diet containing tricin at the rate of 50 ppm and the mice in group 3 were fed an experimental diet containing 250 ppm tricin. Both groups received the experimental diets for 15 wk. The mice in groups 4 (n = 9) received only the 250 ppm tricin-containing diet. The mice in group 5 (n = 9) received only AOM, and the mice in group 6 (n = 9) received only 1.5% DSS in drinking water. The mice of group 7 (n = 9) served as untreated controls.

At week 8, four mice each from groups 1, 2, and 3 and three mice each from groups 4, 5, 6, and 7 were randomly selected and sacrificed to measure mRNA expression of target inflammatory enzymes and cytokines in the colonic mucosa by quantitative reverse transcription-PCR (RT-PCR). At sacrifice, the large bowel of each animal was removed, the contents (feces) were washed out by physiologic saline, and the length from the ileocecal junction to the anal verge were measured. After the large bowels were cut open longitudinally along the main axis and gently washed with saline, scraped colonic mucosa tissue was dipped into the RNAlater solution (Applied Biosystems/Ambion).

At week 18, all of the remaining animals were euthanized by exsanguinations through the abdominal aorta under diethylether anesthesia and subjected to a complete gross necropsy examination to determine the incidence and multiplicity of tumors in the large bowel. At sacrifice, the large bowel was removed and the length was measured. Each large bowel was cut open longitudinally along the main axis and gently washed with saline, then examined manually to determine the incidence and multiplicity of tumors. The colon was fixed in 10% buffered formalin for at least 24 h. Histopathologic examination was done on H&E-stained sections made from paraffin-embedded blocks. Colonic tumors were diagnosed according to criteria established in a prior study (34). The number and density of mucosal ulcers on H&E-stained sections was also recorded.

Immunohistochemistry of proliferating cell nuclear antigen

Immunohistochemical analysis for the proliferating cell nuclear antigen (PCNA) in the colon with or without tumors was done on 4-μm-thick paraffin-embedded sections by the labeled avidin-biotin-peroxidase complex method using a Vectastain ABC kit (Vector Laboratories), with microwave accentuation. The paraffin-embedded sections were heated for 30 min at 65°C, deparaffinized in xylene, and rehydrated with ethanol at room temperature. PBS (pH 7.4; 0.01 mol/L) as used to prepare the solutions and for washes between the preparation steps. Incubations were done in a humidified chamber. The sections were treated for 40 min at room temperature with mouse IgG blocking reagent (Vector Laboratories), and incubated overnight at 4°C with the primary antibody (1:300 dilution; DAKO Japan, Co., Ltd.). The antibody was applied to the sections according to the manufacturer's protocol. Horseradish peroxidase activity was visualized by treatment with H_2O_2 (DAKO Japan, Co., Ltd.) and 3,3'-diaminobenzidine (DAKO Japan) for 5 min. In the last step, the sections were weakly counterstained with Mayer's hematoxylin (Merck). For each examination, negative controls were done on serial sections. The numbers of nuclei with positive reactivity for PCNA-immunohistochemistry were counted by two observers (T.O. and T.T.) who were unaware of the treatment groups to which the slides belonged. The positive rates were evaluated in >100 cancer cells each of 15 different areas of the adenocarcinomas and 10 different crypts of the "normal"-appearing colonic mucosa from five mice each from groups 1 to 3 and expressed as percentage (mean ± SD).

Mitotic index and anaphase bridging index of adenocarcinoma cells

To examine the effects of dietary tricin on chromosomal instability (41) in adenocarcinoma cells, the anaphase bridging index (ABI) was determined on H&E-stained sections. The numbers of mitoses and anaphase bridging were counted in >100 cancer cells from five adenocarcinomas each from groups 1 through 3. The mitotic index (MI; number of mitoses per cancer cells) and ABI (number of anaphases with bridging per mitoses) were expressed as percentages (mean ± SD).

Quantitative RT-PCR

The normal-appearing colonic mucosa of mice from groups 1 through 3 were assayed for mRNA expression of COX-2, iNOS, TNF-α, NF-κB, IκBα, and IKKβ by RT-PCR. RNA was extracted using the RNeasy Mini kit (Qiagen) according to the manufacturer's protocol. cDNA was synthesized from 0.2 μg of total RNA using SuperScript III First-Strand Synthesis System (Invitrogen Co.). Real-time PCR was done in a LightCycler (Roche Diagnostics Co.) with SYBR Premix Ex Taq (TAKARA BIO, INC.). The expression level of each gene was normalized to the β-actin expression level using the standard curve method. Each assay was done six times and the average was calculated. The primers used for amplifications are listed in Supplementary Table S1.

Statistical analysis

Where applicable, data were analyzed using one-way ANOVA with Tukey-Kramer Multiple Comparisons Test or Bonferroni (GraphPad Instat version 3.05, GraphPad Software) with $P < 0.05$ as the limit for statistical significance. Fisher's Exact Probability test or the χ^2 test were used for comparison of the incidence of lesions between the two groups. Data on mRNA expression (mean ± SEM) were analyzed by Mann-Whitney U test.

Results

General observation

All animals remained healthy throughout the experimental period. Food consumption (grams/day/mouse) did not differ significantly among the groups (data not shown). The body weight gains by mice in all of the seven groups were similar during the study (Fig. 1B). The mean body weight of group 2 (AOM/DSS/50 ppm tricin) was significantly lower than that of group 1 ($P < 0.01$; Supplementary Table S2). The mean colon length of group 1 was significantly shorter than the mean

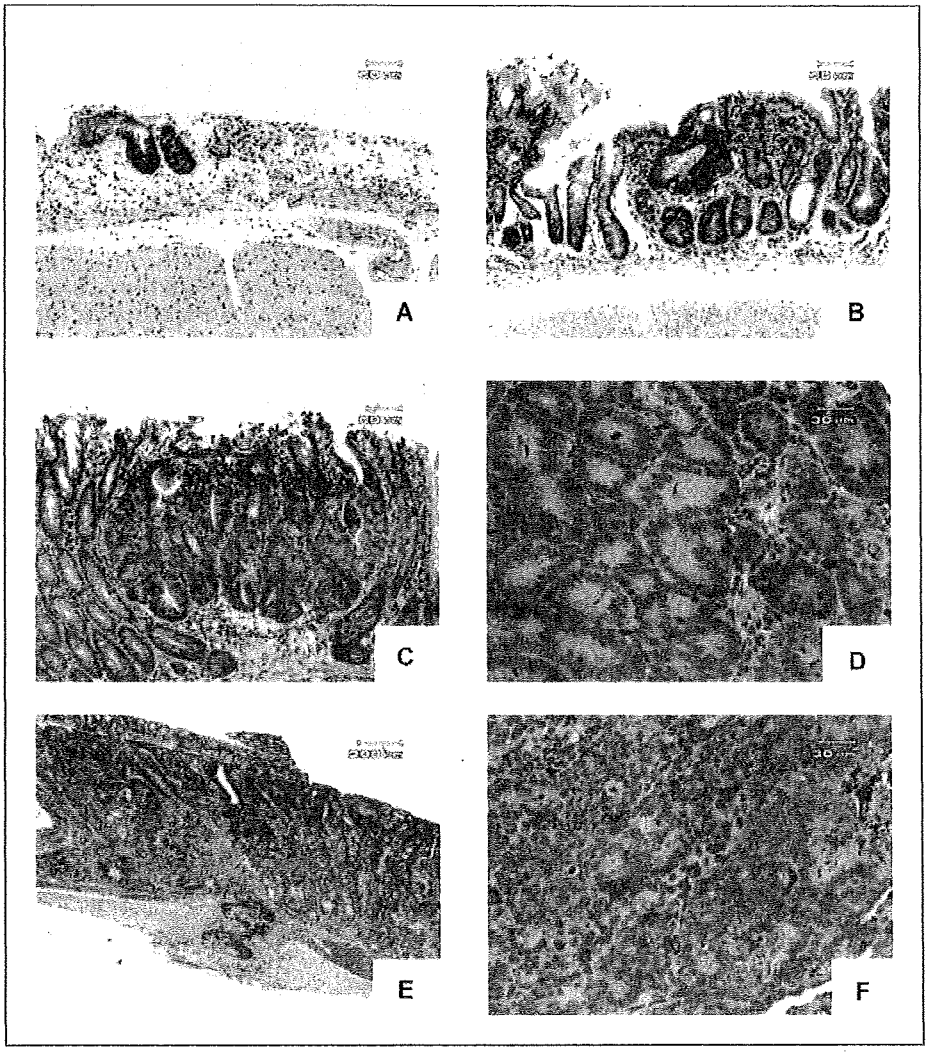

Fig. 2. Representative histopathology of the colonic lesions in group 1 (AOM/DSS). *A*, mucosal ulcer; *B*, dysplastic crypts; *C* and *D*, tubular adenomas; *E* and *F*, moderately differentiated tubular adenocarcinomas.

colon length of group 7 (no treatment; $P < 0.01$; Supplementary Table S2).

Incidence and multiplicity of colonic lesions

The incidence of macroscopic colonic lesions, including tumors and small ulcerations, were seen in the mice in group 1, 2, 3, and 6 (Fig. 1C-E). All mice in groups 1 through 3, which were treated with AOM/DSS with or without tricin, developed colonic tumors (adenoma and/or adenocarcinoma). The mice of group 4, 5, and 7 did not develop colonic tumors.

Microscopic examinations revealed various pathologic colonic lesions in mice from groups 1, 2, 3, and 6. The lesions included mucosal ulcers (Fig. 2A), dysplastic crypts (Fig. 2B), tubular adenomas (Fig. 2C and D), and tubular adenocarcinomas (Fig. 2E and F). Some of the adenocarcinomas that developed in the group 1 mice invaded the subserosa of the colon (Fig. 2E). Table 1 summarizes the microscopic data on the incidence and multiplicity of colonic lesions. The dietary administration of 50 ppm tricin (group 2) significantly reduced the incidence ($P = 0.0117$) and multiplicity ($P < 0.05$) of adenomas and the number of total tumors (adenoma + adenocarcinoma, $P < 0.05$) when compared with group 1. Feeding with 250 ppm tricin (group 3) also significantly lowered the numbers of adenocarcinomas and total tumors when compared with group 1 ($P < 0.05$ for each comparison). The mean numbers of dysplastic crypts in groups 2 ($P < 0.05$) and 3 ($P < 0.01$) were significantly lower than that of dysplastic crypts in group 1. The mean numbers of mucosal ulcers in group 2 ($P < 0.05$) and 3 ($P < 0.001$) were also significantly smaller than that of group 1.

PCNA labeling indices of the normal-appearing crypts and adenocarcinomas

The data on the proliferative kinetics in the normal-appearing crypts and colonic adenocarcinomas by estimating the PCNA labeling indices are shown in Fig. 3. The dietary administration of tricin significantly lowered the PCNA labeling index of the normal-appearing crypts in group 2 (38 ± 11, $P < 0.05$) and group 3 (36 ± 12, $P < 0.05$) when compared with group 1 (48 ± 11). The PCNA labeling indices for colonic adenocarcinomas in groups 2 (74 ± 6, $P < 0.05$) and 3 (71 ± 4, $P < 0.001$) were significantly lower than in group 1 (80 ± 8).

Table 1. Incidence and multiplicity of colonic lesions

Group no.	Treatment (no. of mice examined)	Mucosal ulcer	Dysplasia (high grade)	Adenoma	Adenocarcinoma	Total tumors (AD+ADC)
1	AOM/1.5% DSS (16)	100% (2.69 ± 0.95)*	100% (5.00 ± 3.79)	88% (4.19 ± 4.22)	94% (4.63 ± 3.74)	94% (8.81 ± 6.21)
2	AOM/1.5% DSS/50 ppm tricin (16)	94% (1.81 ± 1.11)	80% (2.56 ± 1.79)†,‡	44%§ (1.44 ± 1.79)†,‡	75% (3.19 ± 2.64)	75% (4.63 ± 4.05)†,‡
3	AOM/1.5% DSS/250 ppm tricin (15)	60% (0.87 ± 0.83)‖	73% (1.53 ± 1.13)¶	67% (1.87 ± 1.73)	67% (1.80 ± 2.04)†,‡	80% (3.67 ±3.37)†,‡
4	250 ppm tricin (6)	0%	0%	0%	0%	0%
5	AOM (6)	0%	0%	0%	0%	0%
6	1.5% DSS (6)	33% (0.33 ± 0.52)	0%	0%	0%	0%
7	None (6)	0%	0%	0%	0%	0%

Abbreviations: AD, adenoma; ADC, adenocarcinoma.
*Mean ± SD.
†Significantly different from group 1 by one-way ANOVA, and Tukey-Kramer Multiple Comparisons test.
‡$P < 0.05$.
§Significantly different from group 1 by Fisher's exact probability test ($P = 0.0117$).
‖$P < 0.001$.
¶$P < 0.01$.

The effects of tricin on the MI and ABI

Dietary administration with tricin affected the number of mitosis (Fig. 4A) and anaphase bridging (Fig. 4B) in adenocarcinomas. As illustrated in Fig. 4C, dietary feeding with tricin significantly decreased the MI in group 2 (17.4 ± 0.9, $P < 0.05$) and group 3 (12.7 ± 2.0, $P < 0.001$) compared with group 1 (20.8 ± 2.4). The treatment also lowered the ABI in group 2 (0.50 ± 0.24) and group 3 (0.29 ± 0.10, $P < 0.05$) compared with group 1 (1.10 ± 0.57).

Expressions of inflammatory enzyme and cytokine genes in colonic mucosa

At week 8, we assayed mRNA levels of COX-2, iNOS, TNF-α, NF-κB, IκBα, and IKKβ in the nonlesional colonic mucosa of

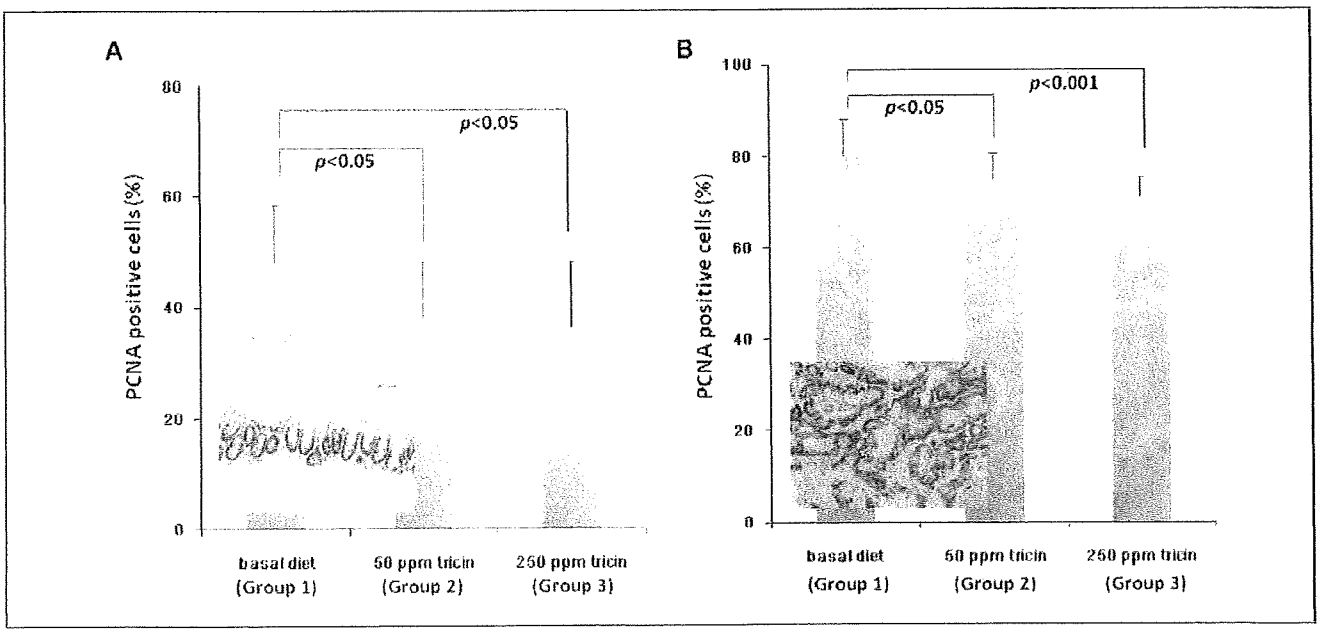

Fig. 3. The PCNA labeling indices of the normal-appearing crypts (*A*) and adenocarcinomas (*B*). Feeding with tricin (groups 2 and 3) significantly lowered the PCNA labeling indices of the normal-appearing crypts ($P < 0.05$ for each comparison) and adenocarcinomas (group 2, $P < 0.05$; and group 3, $P < 0.001$) compared with group 1.

mice in groups 1 through 3 by semiquantitative real-time RT-PCR (Fig. 5). The TNF-α expression significantly decreased in group 3 compared with group 1 ($P < 0.05$; Fig. 5A). Feeding with tricin did not significantly affect the expression of COX-2 (Fig. 5B), iNOS (Fig. 5C), NF-κB (Fig. 5D), IκBα (Fig. 5E), and IKKβ (Fig. 5F).

Discussion

The results described herein clearly indicate that dietary administration with tricin at two dose levels (50 and 250 ppm) significantly inhibited AOM/DSS-induced colonic tumorigenesis in male ICR mice. The high dose (250 ppm) of tricin significantly inhibited development of adenocarcinomas induced by AOM followed by DSS in mice. The dietary administration with tricin also significantly affected the expression of TNF-α in the colonic mucosa at week 8. The treatment resulted in the reduction of the PCNA labeling index, MI, and ABI in the colonic epithelial malignancies at week 18.

The antitumor and chemoprevention activities of tricin have been reported in both *in vitro* and *in vivo* studies. *In vivo* experiments included transplanted human breast cancer cell lines in nude mice (21). In addition, Cai et al. reported that 0.2% tricin in diet effectively inhibited the number of adenomas in the small intestine of $Apc^{Min/+}$ mice (42). They did not, however, observe inhibition of the development of colonic tumors (42). In the current study, we observed the cancer chemopreventive activity of dietary tricin in carcinogenesis in the inflamed colon. In addition, feeding with tricin lowered the occurrence of mucosal ulcers and preneoplasms (dysplastic crypts).

We can point several mechanisms by which tricin may suppress AOM/DSS-induced colon carcinogenesis in this study. Our findings that dietary tricin lowered the PCNA labeling index, MI, and ABI of colonic adenocarcinomas may suggest an antigrowth effect of tricin on colonic malignancy. The findings are in agreement with the reports by Cai et al. (21) that showed tricin or tricin-containing extracts of brown rice inhibited the growth of the colon and mammary cells *in vitro* and *in vivo* (22). In addition, the results that dietary tricin lowered the ABI of adenocarcinoma cells suggest that tricin affects the chromosomal instability of cancer cells and possibly their telomerase activity (41). Tricin may exert chemopreventive activity through inhibition of COX-1 and 2 enzymes and prostaglandin E_2 production in human colon cancer cell lines (HT-29 and HCA-7) and the small intestine of $Apc^{Min/+}$ mice (23, 24). Unexpectedly, dietary tricin did not significantly alter the expression of COX-2 or iNOS at week 8. The suppression of NF-κB–signaling pathway by dietary administration with tricin was insignificant. However,

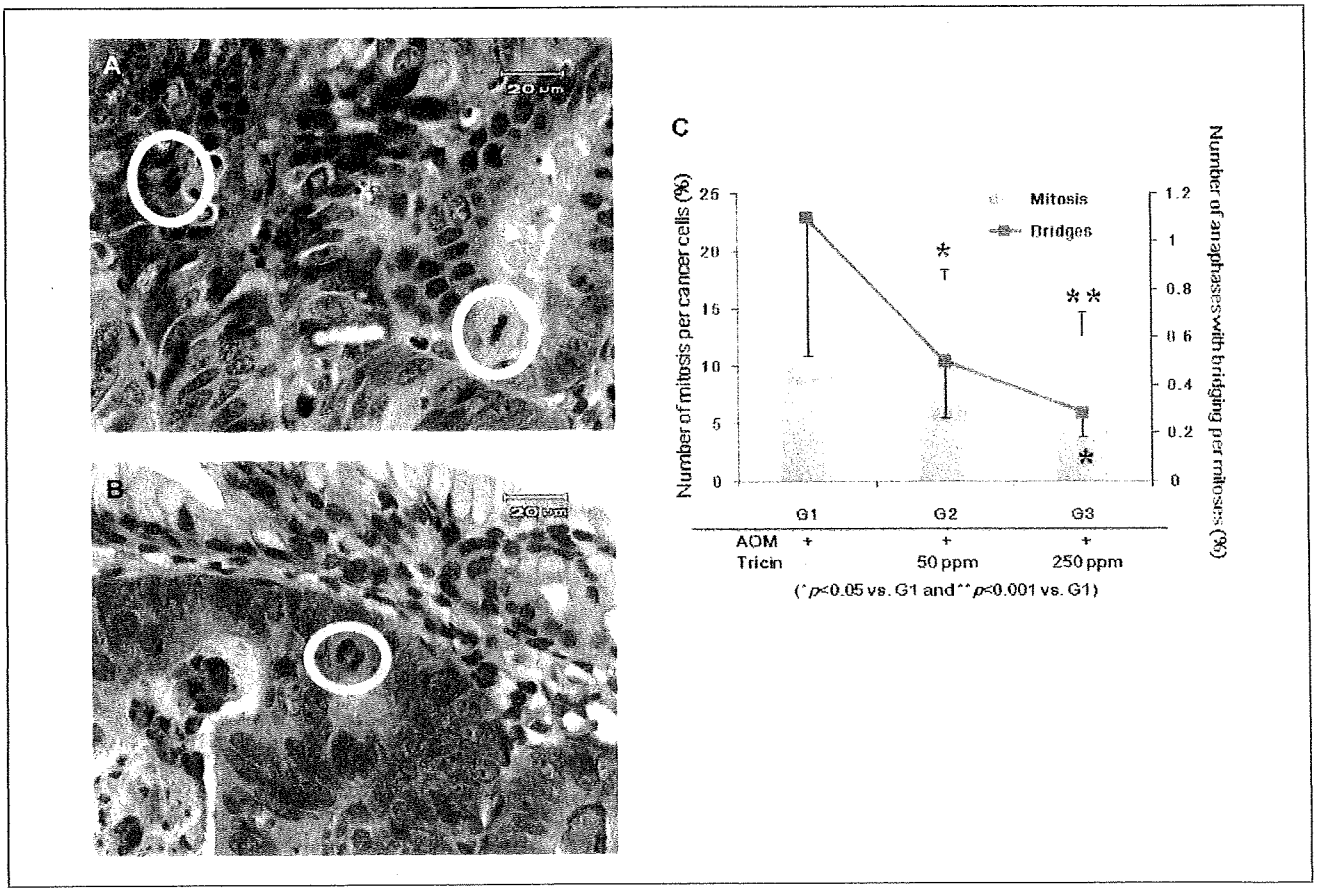

Fig. 4. The effects of dietary tricin on the MI and ABI. *A*, representative mitotic figures (*left circle*, anaphase; *right circle*, metaphase) in an adenocarcinoma, (*B*) representative anaphase bridging (*circle*) in an adenocarcinoma, and (C) MI (*columns*) and ABI (*lines*). Dietary administration of tricin significantly reduced the MI (50 ppm tricin, $P < 0.05$; and 250 ppm tricin, $P < 0.001$) and ABI (250 ppm tricin, $P < 0.05$). *G1*, group1; *G2*, group2; and *G3*, group 3.

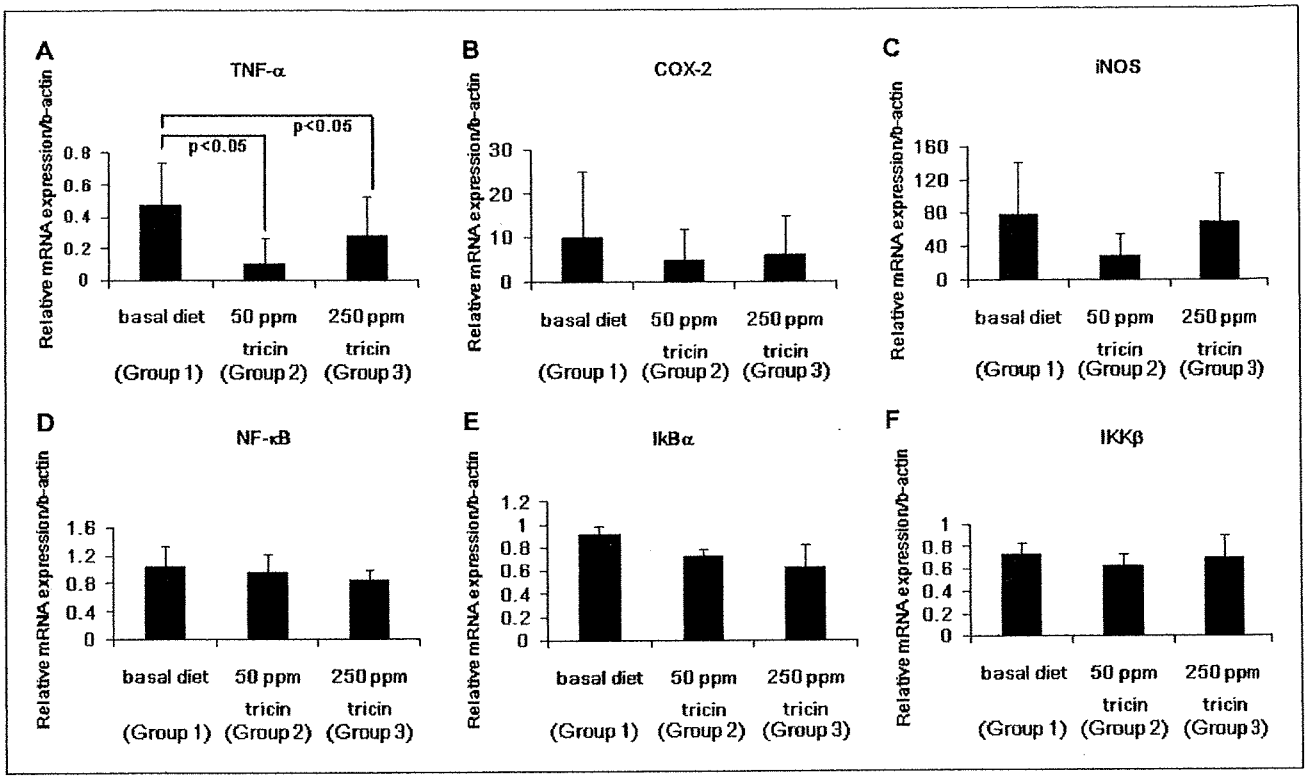

Fig. 5. The expression of (*A*) TNF-α (*B*) COX-2, (*C*) iNOS, (*D*) NF-κB, (*E*) IκBα, and (*F*) IKKβ in the normal-appearing colonic mucosa of groups 1 to 3 that were assessed by semiquantitative real-time RT-PCR. The expression of TNF-α was significantly inhibited by feeding with tricin (groups 2 and 3, $P < 0.05$ for each comparison). Feeding with tricin lowered the expression of COX-2, iNOS, and the NF-κB signaling pathway, but the reduction did not reach statistical significance. The expression was normalized to β-actin mRNA expression. Samples were analyzed in triplicate. *Columns*, mean of three independent experiments; *bars*, SEM; $n = 12$, Statistical analysis was done by the Mann-Whitney *U* test.

we observed that dietary tricin significantly inhibited the expression of TNF-α in the nonlesions colonic mucosa. Such effects are of interest because TNF-α acts as a master switch to establish an intricate link between inflammation and cancer (39, 40).

In conclusion, the dietary administration with tricin effectively suppressed AOM/DSS-induced colon carcinogenesis by suppressing the expression of TNF-α in the early phase and MI and ABI in the later phase. The effects of tricin on TNF-α expression are also important in the chemopreventive activity of tricin in inflammation-associated colorectal carcinogenesis. The safety of tricin was reported by Verschoyle et al. (43). A natural flavonoid tricin is present in edible plants, including rice, oats, barley, and wheat (10). In the current study, we isolated tricin from the dried leaves of *Sasa albo-marginata* that contain a large amount (0.2 ppm) of tricin than rice (Oryza sativa L.; 0.066 ppm). Tricin is thus a candidate for clinical use for fighting colorectal cancer development in patients without colitis.

Disclosure of Potential Conflicts of Interest

No potential conflicts of interest were disclosed.

References

1. Jemal A, Siegel R, Ward E, et al. Cancer statistics, 2008. CA Cancer J Clin 2008;58:71–96.
2. Karim-Kos HE, de Vries E, Soerjomataram I, Lemmens V, Siesling S, Coebergh JW. Recent trends of cancer in Europe: a combined approach of incidence, survival and mortality for 17 cancer sites since the 1990s. Eur J Cancer 2008;44:1345–89.
3. Tanaka T. Colorectal carcinogenesis: review of human and experimental animal studies. J Carcinog 2009;8:5.
4. Rosenberg DW, Giardina C, Tanaka T. Mouse models for the study of colon carcinogenesis. Carcinogenesis 2009;30:183–96.
5. Tanaka T. Effect of diet on human carcinogenesis. Crit Rev Oncol Hematol 1997;25:73–95.
6. Tanaka T, Miyamoto S, Suzuki R, Yasui Y. Chemoprevention of colon carcinogenesis by dietary nonnutritive compounds. Curr Top Neutraceut Res 2006;4:127–52.
7. Tanaka T, Oyama T, Yasui Y. Dietetary supplements and colorectal cancer. Curr Topics Neutarceut Res 2008;6:165–88.
8. Murthy NS, Mukherjee S, Ray G, Ray A. Dietary factors and cancer chemoprevention: an overview of obesity-related malignancies. J Postgrad Med 2009;55:45–54.
9. Pan MH, Ho CT. Chemopreventive effects of natural dietary compounds on cancer development. Chem Soc Rev 2008;37:2558–74.
10. Wang HK, Xia Y, Yang ZY, Natschke SL, Lee KH. Recent advances in the discovery and development of flavonoids and their analogues as antitumor and anti-HIV agents. Adv Exp Med Biol 1998;439:191–225.
11. Park HS, Lim JH, Kim HJ, Choi HJ, Lee IS. Antioxidant flavone glycosides from the leaves of Sasa borealis. Arch Pharm Res 2007;30:161–6.
12. Fiorentino A, D'Abrosca B, Pacifico S, et al. Potential allelopatic effects of stilbenoids and flavonoids from leaves of Carex distachya Desf. Biochem Syst Ecol 2008;36:691–8.
13. Duarte-Almeida JM, Negri G, Salatino A, de Carvalho JE, Lajolo FM. Antiproliferative and antioxidant activities of a tricin acylated glycoside from sugarcane (Saccharum officinarum) juice. Phytochemistry 2007;68:1165–71.

14. Renuka Devi R, Arumughan C. Antiradical efficacy of phytochemical extracts from defatted rice bran. Food Chem Toxicol 2007;45:2014–21.
15. Sakai A, Watanabe K, Koketsu M, et al. Anti-human cytomegalovirus activity of constituents from Sasa albo-marginata (Kumazasa in Japan). Antivir Chem Chemother 2008;19:125–32.
16. Kuwabara H, Mouri K, Otsuka H, Kasai R, Yamasaki K. Tricin from a malagasy connaraceous plant with potent antihistaminic activity. J Nat Prod 2003;66:1273–5.
17. Aggarwal BB, Shishodia S. Molecular targets of dietary agents for prevention and therapy of cancer. Biochem Pharmacol 2006;71:1397–421.
18. Janakiram NB, Rao CV. Molecular markers and targets for colorectal cancer prevention. Acta Pharmacol Sin 2008;29:1–20.
19. Surh YJ. Cancer chemoprevention with dietary phytochemicals. Nat Rev Cancer 2003;3:768–80.
20. Yasui Y, Kim M, Oyama T, Tanaka T. Colorectal carcinogenesis and suppression of tumor development by inhibition of enzymes and molecular targets. Curr Enzyme Inhibition 2009;5:1–26.
21. Cai H, Hudson EA, Mann P, et al. Growth-inhibitory and cell cycle-arresting properties of the rice bran constituent tricin in human-derived breast cancer cells *in vitro* and in nude mice *in vivo*. Br J Cancer 2004;91:1364–71.
22. Hudson EA, Dinh PA, Kokubun T, Simmonds MS, Gescher A. Characterization of potentially chemopreventive phenols in extracts of brown rice that inhibit the growth of human breast and colon cancer cells. Cancer Epidemiol Biomarkers Prev 2000;9:1163–70.
23. Cai H, Al-Fayez M, Tunstall RG, et al. The rice bran constituent tricin potently inhibits cyclooxygenase enzymes and interferes with intestinal carcinogenesis in ApcMin mice. Mol Cancer Ther 2005;4:1287–92.
24. Al-Fayez M, Cai H, Tunstall R, Steward WP, Gescher AJ. Differential modulation of cyclooxygenase-mediated prostaglandin production by the putative cancer chemopreventive flavonoids tricin, apigenin and quercetin. Cancer Chemother Pharmacol 2006;58:816–25.
25. Cai H, Boocock DJ, Steward WP, Gescher AJ. Tissue distribution in mice and metabolism in murine and human liver of apigenin and tricin, flavones with putative cancer chemopreventive properties. Cancer Chemother Pharmacol 2007;60:257–66.
26. Cai H, Brown K, Steward WP, Gescher AJ. Determination of 3′,4′,5′,5,7-pentamethoxyflavone in the plasma and intestinal mucosa of mice by HPLC with UV detection. Biomed Chromatogr 2009;23:335–9.
27. Cai H, Steward WP, Gescher AJ. Determination of the putative cancer chemopreventive flavone tricin in plasma and tissues of mice by HPLC with UV-visible detection. Biomed Chromatogr 2005;19:518–22.
28. Cai H, Verschoyle RD, Steward WP, Gescher AJ. Determination of the flavone tricin in human plasma by high-performance liquid chromatography. Biomed Chromatogr 2003;17:435–9.
29. Tanaka T, Yasui Y, Ishigamori-Suzuki R, Oyama T. Citrus compounds inhibit inflammation- and obesity-related colon carcinogenesis in mice. Nutr Cancer 2008;60 Suppl 1:70–80.
30. Tanaka T, Yasui Y, Tanaka M, Oyama T, Rahman KM. Melatonin suppresses AOM/DSS-induced large bowel oncogenesis in rats. Chem Biol Interact 2009;177:128–36.
31. Suzuki R, Kohno H, Sugie S, Tanaka T. Sequential observations on the occurrence of preneoplastic and neoplastic lesions in mouse colon treated with azoxymethane and dextran sodium sulfate. Cancer Sci 2004;95:721–7.
32. Suzuki R, Kohno H, Sugie S, Tanaka T. Dose-dependent promoting effect of dextran sodium sulfate on mouse colon carcinogenesis initiated with azoxymethane. Histol Histopathol 2005;20:483–92.
33. Tanaka T, Kohno H, Suzuki R, et al. Dextran sodium sulfate strongly promotes colorectal carcinogenesis in Apc(Min/+) mice: inflammatory stimuli by dextran sodium sulfate results in development of multiple colonic neoplasms. Int J Cancer 2006;118:25–34.
34. Tanaka T, Kohno H, Suzuki R, Yamada Y, Sugie S, Mori H. A novel inflammation-related mouse colon carcinogenesis model induced by azoxymethane and dextran sodium sulfate. Cancer Sci 2003;94:965–73.
35. Reddy BS. Studies with the azoxymethane-rat preclinical model for assessing colon tumor development and chemoprevention. Environ Mol Mutagen 2004;44:26–35.
36. Reddy BS, Rao CV. Chemoprophylaxis of colon cancer. Curr Gastroenterol Rep 2005;7:389–95.
37. Rao CV. Regulation of COX and LOX by curcumin. Adv Exp Med Biol 2007;595:213–26.
38. Rao CV. Nitric oxide signaling in colon cancer chemoprevention. Mutat Res 2004;555:107–19.
39. Sethi G, Sung B, Aggarwal BB. TNF: a master switch for inflammation to cancer. Front Biosci 2008;13:5094–107.
40. Aggarwal BB, Shishodia S, Sandur SK, Pandey MK, Sethi G. Inflammation and cancer: how hot is the link? Biochem Pharmacol 2006;72:1605–21.
41. Rudolph KL, Millard M, Bosenberg MW, DePinho RA. Telomere dysfunction and evolution of intestinal carcinoma in mice and humans. Nat Genet 2001;28:155–9.
42. Yamada Y, Hata K, Hirose Y, et al. Microadenomatous lesions involving loss of Apc heterozygosity in the colon of adult Apc(Min/+) mice. Cancer Res 2002;62:6367–70.
43. Verschoyle RD, Greaves P, Cai H, et al. Preliminary safety evaluation of the putative cancer chemopreventive agent tricin, a naturally occurring flavone. Cancer Chemother Pharmacol 2006;57:1–6.

Int. J. Cancer: **125**, 1786–1795 (2009)

Anti-inflammatory effects of caffeic acid phenethyl ester (CAPE), a nuclear factor-κB inhibitor, on *Helicobacter pylori*-induced gastritis in Mongolian gerbils

Takeshi Toyoda[1], Tetsuya Tsukamoto[1]*, Shinji Takasu[1], Liang Shi[1], Naoki Hirano[1], Hisayo Ban[1], Toshiko Kumagai[2] and Masae Tatematsu[1,3]

[1]*Division of Oncological Pathology, Aichi Cancer Center Research Institute, Chikusa-ku, Nagoya, Japan*
[2]*Central Clinical Laboratories, Shinshu University Hospital, Matsumoto, Nagano, Japan*
[3]*Division of Cancer Genetics, Nagoya University Graduate School of Medicine, Showa-ku, Nagoya, Japan*

Nuclear factor-κB (NF-κB) plays a major role in host inflammatory responses and carcinogenesis and as such is an important drug target for adjuvant therapy. In this study, we examined the effect of caffeic acid phenethyl ester (CAPE), an NF-κB inhibitor, on *Helicobacter pylori* (*H. pylori*)-induced NF-κB activation in cell culture and chronic gastritis in Mongolian gerbils. In AGS gastric cancer cells, CAPE significantly inhibited *H. pylori*-stimulated NF-κB activation and mRNA expression of several inflammatory factors in a dose-dependent manner, and prevented degradation of IκB-α and phosphorylation of p65 subunit. To evaluate the effects of CAPE on *H. pylori*-induced gastritis, specific pathogen-free male, 6-week-old Mongolian gerbils were intragastrically inoculated with *H. pylori*, fed diets containing CAPE (0–0.1%) and sacrificed after 12 weeks. Infiltration of neutrophils and mononuclear cells and expression of NF-κB p50 subunit and phospho-IκB-α were significantly suppressed by 0.1% CAPE treatment in the antrum of *H. pylori*-infected gerbils. Labeling indices for 5′-bromo-2′-deoxyuridine both in the antrum and corpus and lengths of isolated pyloric glands were also markedly reduced at the highest dose, suggesting a preventive effect of CAPE on epithelial proliferation. Furthermore, in the pyloric mucosa, mRNA expression of inflammatory mediators including tumor necrosis factor-α, interferon-γ, interleukin (IL)-2, IL-6, KC (IL-8 homologue), and inducible nitric oxide synthase was significantly reduced. These results suggest that CAPE has inhibitory effects on *H. pylori*-induced gastritis in Mongolian gerbils through the suppression of NF-κB activation, and may thus have potential for prevention and therapy of *H. pylori*-associated gastric disorders.
© *2009 UICC*

Key words: *Helicobacter pylori*; caffeic acid phenethyl ester; chemoprevention; gastritis; Mongolian gerbils

Nuclear factor-κB (NF-κB) plays a central role in many physiological processes in the whole body such as immune responses, cell proliferation, and inflammation through promoting transcription of various cytokines, enzymes, chemokines, antiapoptotic factors and cell growth factors.[1] Because many types of cancer, including neoplasm in the stomach, are known to be associated with chronic inflammation,[2] inhibition of NF-κB activation has attracted increasing attention as a new therapeutic approach for chemoprevention of cancer development.[3,4] Several natural and synthetic compounds have been found to inhibit NF-κB activation, and to exert anti-inflammatory effects *in vitro* and *in vivo*.[5,6] Caffeic acid phenethyl ester (CAPE), one of the active components of propolis derived from honeybee hives, has been reported to be a selective inhibitor of NF-κB.[7,8] Besides that, recent study has also shown that CAPE may inhibit activator protein-1 (AP-1) activity in *Helicobacter pylori* (*H. pylori*)-stimulated gastric epithelial cells.[9] Thus, further investigation was needed, to confirm how CAPE would influence many signal transduction cascades other than NF-κB pathway. Although the mechanisms of NF-κB inhibition by CAPE are not fully understood, research has demonstrated anti-inflammatory, anticarcinogenic and immunomodulatory effects of the compound in animal models.[10–12]

H. pylori is now recognized as a major causative factor for chronic gastritis and peptic ulcer, and there is compelling evidence indicating an association between *H. pylori*-induced chronic gastritis and development of stomach cancer.[13,14] Triple therapy with a proton pump inhibitor and 2 antimicrobials, amoxicillin and clarithromycin, is usually recommended as the general therapy for *H. pylori* eradication.[15] However, considering the occurrence of antibiotic-resistance, the search for new agents for alternative therapies continues to be very important.[16] *H. pylori* infection also leads to activation of NF-κB signaling in gastric epithelial cells, and NF-κB-mediated cytokine expression is essentially involved with *H. pylori*-induced gastritis.[17–21] Thus the degree of gastritis induced by a mutant strain of *H. pylori* lacking capacity for NF-κB activation was found to be lower than that with wild type infection.[22] Inhibition of NF-κB could be a promising target for prevention and adjuvant therapy of *H. pylori*-associated gastric disorders.[3,23]

The Mongolian gerbil (*Meriones unguiculatus*) provides a useful animal model of *H. pylori*-induced chronic active gastritis, allowing investigation of morbidity-related epithelial alterations in the gastric mucosa and their development into gastric neoplasia.[24] We have previously demonstrated that some natural products in food such as a fruit-juice concentrate of Japanese apricot and nordihydroguaiaretic acid, an antioxidant to preserve food and oils, and canolol, a potent oxygen radicals scavenger contained in canola oil, have suppressive effects on *H. pylori*-induced gastric disorders in Mongolian gerbils.[25–27] The purpose of this study was to evaluate possible anti-inflammatory effects of CAPE, a naturally-occurring compound in food, in the same model.

Material and methods

Chemicals and cell culture

CAPE was purchased from Cayman Chemicals (Ann Arbor, MI) (Fig. 1). AGS cells, the human gastric cancer cell line, were maintained in RPMI 1640 medium (Gibco, Grand Island, NY) supplemented with 10% heat-inactivated fetal calf serum (FCS, Sigma Chemical, St. Louis, MO), penicillin (100 units/ml), streptomycin (100 μg/ml) and amphotericin B (0.25 μg/ml) (Invitrogen, Carlsbad, CA). Culture dishes and plates were kept in an incubator with a humidified atmosphere of 5% CO_2 at 37°C. CAPE was

Abbreviations: AI, arbitrary index; AP-1, activator protein-1; BrdU, 5′-bromo-2′-deoxyuridine; CAPE, caffeic acid phenethyl ester; CFU, colony-forming units; COX, cyclooxygenase; EDTA, ethylenediaminetetraacetic acid; FCS, fetal calf serum; GAPDH, glyceraldehyde-3-phosphate dehydrogenase; H&E, hematoxylin and eosin; *H. pylori*, *Helicobacter pylori*; HBSS, Hanks' balanced salt solution; IFN, interferon; IL, interleukin; iNOS, inducible nitric oxide synthase; NF-κB, nuclear factor-κB; TNF, tumor necrosis factor.

Grant sponsors: Third-term Comprehensive 10-year Strategy for Cancer Control, Ministry of Health, Labour and Welfare, Ministry of Education, Culture, Sports, Science and Technology.

***Correspondence to:** Division of Oncological Pathology, Aichi Cancer Center Research Institute, 1-1 Kanokoden, Chikusa-ku, Nagoya 464-8681, Japan. Fax: +81-52-764-2972. E-mail: ttsukamt@aichi-cc.jp

Received 19 November 2008; Accepted after revision 27 April 2009
DOI 10.1002/ijc.24586
Published online 18 May 2009 in Wiley InterScience (www.interscience.wiley.com).

prepared as a 20 mg/ml solution in dimethyl sulfoxide immediately before use.

Bacterial culture

H. pylori was prepared by the same method as described previously.[28] Briefly, *H. pylori* strain ATCC43504 (American Type Culture Collection, Rockville, MD) was grown in Brucella broth (Becton Dickinson, Cockeysville, MD) containing 7% FCS, at 37°C under microaerobic conditions using an Anaero Pack Campylo (Mitsubishi Gas Chemical, Tokyo, Japan), at high humidity for 24 hr. The broth cultures of *H. pylori* were checked under a phase contrast microscope for bacterial shape and motility.

Luciferase reporter assay on transcriptional activation of NF-κB

To assess whether NF-κB is activated by *H. pylori* infection in gastric cancer cells and to determine the effects of CAPE, luciferase reporter assays were performed. AGS cells were cotransfected in a 24-well culture plate with two expression plasmids, one including a luciferase reporter gene under transcriptional control of the NF-κB element (pNF-κB-Luc; Stratagene, La Jolla, CA)

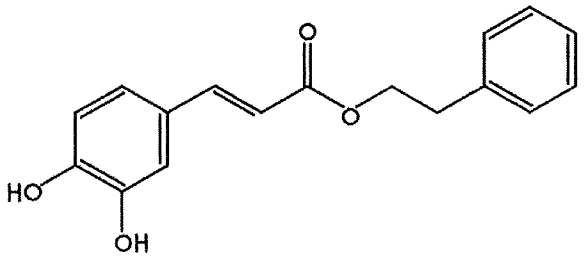

FIGURE 1 – Chemical structure of caffeic acid phenethyl ester. $C_{17}H_{16}O_4$, molecular weight 284.3.

and the other a transfection efficiency indicator (pGL4.74[*hRluc*/TK] Vector; Promega, Madison, WI) using the Lipofectamin 2000 (Invitrogen) transfection reagent. After 24 hr incubation, cells were challenged by infection with 1×10^6 colony-forming units (CFU)/well of *H. pylori* and immediately treated with various concentrations of CAPE (0, 10, 20, or 40 μg/ml) for 24 hr. NF-κB luciferase reporter gene assays were performed with a Dual Luciferase Reporter Assay System (Promega) and a luminometer (Lumat LB9501; Berthold, Bad Wildbad, Germany) according to the manufacturer's instructions.

Analysis of mRNA expression for inflammatory factors by relative quantitative real-time RT-PCR

To investigate the effects of CAPE on cytokine expression of *H. pylori*-stimulated AGS cells, real-time RT-PCR analysis was performed. AGS cells were challenged by infection with 1×10^7 colony-forming units (CFU)/dish of *H. pylori* and immediately treated with CAPE (0, 5, 10 or 20 μg/ml). After 24 hr incubation, total RNA was extracted from these cells using an RNeasy Plus Mini Kit (Qiagen, Hilden, Germany). After DNase treatment, first strand cDNAs were synthesized using a SuperScript III First-Strand Synthesis System (Invitrogen) according to the manufacturer's instructions. Relative quantitative PCR of tumor necrosis factor-α (TNF-α), interleukin (IL)-1β, IL-8, IL-10, inducible nitric oxide synthase (iNOS) and cyclooxygenase-2 (COX-2) was carried out using a LightCycler system (Roche Diagnostics, Mannheim, Germany) with the glyceraldehyde-3-phosphate dehydrogenase (GAPDH) gene as an internal control. The PCR was performed basically as described earlier using a QuantiTect SYBR Green PCR Kit (Qiagen).[29] The primer sequences for each marker are listed in Table I. Specificity of the PCR reaction was confirmed using the melting program provided with the LightCycler software. To further confirm that there was no obvious primer dimer formation or amplification of any extra bands, the samples were electrophoresed in 3% agarose gels and visualized with ethidium bromide after the LightCycler reaction. Relative quantifica-

TABLE I – PRIMER SEQUENCES FOR RELATIVE QUANTITATIVE REAL-TIME RT-PCR

Species	Gene	Sequences	Product length (bp)	Accession no.
Gerbil	GAPDH	5′-AACGGCACAGTCAAGGCTGAGAACG-3′ 5′-CAACATACTCGGCACCGGCATCG-3′	118	AB040445
	TNF-α	5′-GCCCCCACCTCGTGCTCCTCAC-3′ 5′-GGCAGGGGCTCTTGATGGCAGACAG-3′	96	AB177841
	IFN-γ	5′-AGAGCATAAACGCCATCAGG-3′ 5′-TGCTCTGGATCTGTGGATCA-3′	120	L37782
	IL-2	5′-AGCTCCTGAGAGGGATCAAC-3′ 5′-ACATCATGCAGAGGTCCAAG-3′	139	X68779
	IL-6	5′-ATGGCTGAAGTCCAAGACC-3′ 5′-GGAATGTCCTCAGCTTGGTA-3′	125	AB164706
	IL-10	5′-CAGGGCTCCTGAAAGAGTTA-3′ 5′-AGAATGAGGTCAGGGGAATC-3′	114	L37781
	iNOS	5′-GCTTGAGCGAGGAGCAGGTTGAGGA-3′ 5′-CGCTGGCCTTTTTCACCCCATAGGA-3′	111	AB177843
	KC	5′-CACCCGCTCGCTTCTTC-3′ 5′-ATGCTCTTGGGGTGAATCC-3′	138	AJ877921
Human	GAPDH	5′-GGGAAGCTTGTCATCAATGG-3′ 5′-TGGACTCCACGACGTACTCA-3′	103	NM_002046
	TNF-α	5′-AGCCCATGTTGTAGCAAACC-3′ 5′-ATGAGGTACAGGCCCTCTGA-3′	135	AF043342
	IL-1β	5′-AGGGACAGGATATGGAGCAA-3′ 5′-TTCAACACGCAGGACAGGTA-3′	127	NM_000576
	IL-8	5′-CGGAAGGAACCATCTCACTG-3′ 5′-AGCACTCCTTGGCAAAACTG-3′	116	NM_000584
	IL-10	5′-CCAAGACCCAGACATCAAGG-3′ 5′-GGCCTTGCTCTTGTTTTCAC-3′	115	NM_000572
	iNOS	5′-CCCAAGCTCTACACCTCCAA-3′ 5′-TTTGAGCCTCATGGTGAACA-3′	132	AB022318
	COX-2	5′-CGCTTTATGCTGAAGCCCTA-3′ 5′-TTTCTACCAGAAGGGCAGGA-3′	127	M90100

GAPDH, glyceraldehyde-3-phosphate dehydrogenase; TNF, tumor necrosis factor; IFN, interferon; IL, interleukin; iNOS, inducible nitric oxide synthase; COX, cyclooxygenase.

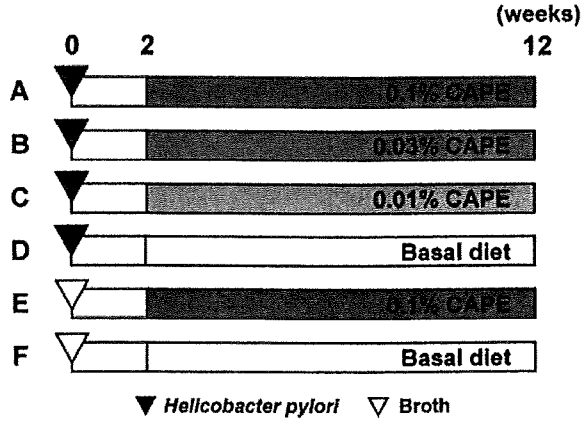

FIGURE 2 – Experimental design. Six-week-old male Mongolian gerbils were inoculated with *Helicobacter pylori* (ATCC43504 strain) or Brucella broth. After 2 weeks, animals were given basal diets (CE-2) containing caffeic acid phenethyl ester (CAPE) at various concentrations (0, 0.01, 0.03 and 0.1%) for 10 weeks.

tion was performed as previously established using the internal control without the necessity for external standards.[29]

Western blot analysis

Total protein extract was obtained from *H. pylori*-stimulated and CAPE-treated AGS cells by a Nuclear Extract Kit (Active Motif, Carlsbad, CA). Protein samples were fractionated by SDS-PAGE and electrophoretically transferred to a PVDF membrane. Blots were blocked with 5% nonfat dry milk in tris-buffered saline for 1 hr and then incubated over night with a rabbit polyclonal anti-IκB-α antibody (Cell Signaling Technology, Beverly, MA), a mouse monoclonal anti-α-tubulin antibody (clone DM1A, Santa Cruz Biotechnology, Santa Cruz, CA), a rabbit polyclonal anti-phospho-NF-κB p65 antibody (Ser276, Cell Signaling Technology) and a mouse monoclonal anti-actin antibody (clone ACTN05, Thermo Scientific, Fremont, CA). Detection was performed using an Immun-Star HRP Chemiluminescent Kit (Bio-Rad Laboratories, Hercules, CA).

In vivo *experimental design*

The experimental design is illustrated in Figure 2. A total of 55 specific pathogen-free male, 6-week-old Mongolian gerbils (*Meriones unguiculatus*; MGS/Sea, Kyudo, Fukuoka, Japan) were used. They were housed in plastic cages on hardwood-chip bedding in an air-conditioned biohazard room with a 12-hr light/12-hr dark cycle, and allowed free access to food and water throughout. The gerbils were divided into 6 groups (Groups A–F). Animals of Groups A–D were inoculated with 1.0 ml of broth culture containing *H. pylori* (1×10^8 CFU/ml) intragastrically using an oral catheter, while gerbils of Groups E and F were inoculated with Brucella broth alone. From weeks 2 to 12, the gerbils received CE-2 diets (CLEA Japan, Tokyo, Japan) containing CAPE at the concentrations of 0.1% (Groups A and E), 0.03% (Group B), 0.01% (Group C) and 0% (Groups D and F). All experimental diets were prepared at 8 day intervals in our laboratory and stored in a refrigerator. Food cups were replenished with fresh diet every second day. At week 12, all gerbils were intraperitoneally injected with 5′-bromo-2′-deoxyuridine (BrdU) at a dose of 100 mg/kg, 1 hr before sacrifice. The animals were then subjected to deep anesthesia and laparotomy with excision of the stomach, liver, spleen, kidney, heart and lung, and blood samples were collected from the inferior vena cava. The experimental design was approved by the Animal Care Committee of the Aichi Cancer Center Research Institute, and the animals were cared for in accordance with institutional guidelines as well as the Guidelines for Proper Conduct of Animal Experiments (Science Council of Japan, June 1, 2006).

Histopathology and immunohistochemistry

The excised stomachs were fixed in 10% neutral-buffered formalin for 24 hr and sliced along the longitudinal axis into 4–8 strips of equal width, and embedded in paraffin. Serial paraffin sections were prepared and stained with hematoxylin and eosin (H&E) for morphological observation. The glandular mucosa of the antrum and corpus was examined histologically for inflammation and epithelial changes. The degree of chronic active gastritis was graded according to criteria modified from the Updated Sydney System,[30] by scoring the infiltration of neutrophils and mononuclear cells, intestinal metaplasia and heterotopic proliferative glands, on a four-point scale (0–3; 0, normal; 1, mild; 2, moderate; 3, marked). Epithelial cell proliferation was assessed by BrdU labeling, visualized by immunostaining with a mouse monoclonal anti-BrdU antibody (clone Bu20a, diluted 1:1000, Dako, Glostrup, Denmark) as described previously.[31] Labeling indices in BrdU-stained slides were determined as the mean percentages of BrdU-positive epithelial cells among total cells in 10 different randomly selected glands in both the antrum and corpus. Immunohistochemical analyses were carried out with a mouse monoclonal anti-COX-2 antibody (clone 33, diluted 1:100, BD Biosciences, San Jose, CA), a mouse monoclonal anti-phospho-IκB-α antibody (clone 5A5, diluted 1:150, Cell Signaling Technology) and a rabbit polyclonal anti-NFκB p50 antibody (clone H-119, diluted 1:100, Santa Cruz Biotechnology) as previously described.[32–34] To quantitate the degree of staining, a grading system was employed with the following criteria: grade 0 (negative), grades 1–3 (increasing degrees of intermediate immunoreactivity) and grade 4 (extensive reactivity).

Gland isolation

Gland isolation was performed as previously described.[35] Briefly, remaining portions of resected gastric mucosa were injected with calcium- and magnesium-free Hanks' balanced salt solution (HBSS) containing 30 mM ethylenediaminetetraacetic acid (EDTA) submucosally, incubated in EDTA-HBSS, and shaken for 15 min at 37°C. Then the mucosa was scraped off with a scalpel. Isolated glands were washed in phosphate buffered saline, fixed in 70% ethanol for a few hours, dehydrated with 95% ethanol, and stored at −20°C until use.

Analysis of mRNA expression in the pyloric mucosa of Mongolian gerbils

Relative quantitative real-time RT-PCR for TNF-α, interferon-γ (IFN-γ), IL-2, IL-6, IL-10, iNOS and IL-8 homologue (KC) was carried out using total RNA extracted from selected pyloric mucosal tissue with the gerbil-specific GAPDH gene as an internal control same as above. The expression levels of mRNAs were expressed relative to 1.0 in the control group (Group F).

Serology

Blood samples were centrifuged and separated sera were stored at −80°C until use. The titer of anti-*H. pylori* antibodies was measured using an ELISA kit (Biomerica, Newport Beach, CA) and values were expressed using an arbitrary index (AI).[27] Sera were also used for measurement of gastrin levels (SRL, Tokyo, Japan).

Statistical analysis

Quantitative values were expressed as means ± SD or SE, and differences between means were statistically analyzed by ANOVA or Kruskal-Wallis followed by a multiple comparison test. p values of less than 0.05 were considered to be statistically significant.

Results

Suppressive effects of CAPE on H. pylori*-induced NF-κB activation and mRNA expression of inflammatory factors in AGS cells*

NF-κB activation in *H. pylori*-stimulated AGS cells was significantly increased as compared to that in noninfected control cells ($p < 0.01$) (Fig. 3). CAPE decreased the *H. pylori*-induced NF-κB transcriptional activation in a dose-dependent manner, with significance at the 20 and 40 μg/ml doses ($p < 0.05$ and $p < 0.01$, respectively). Relative quantitative real time RT-PCR data for mRNA expression of inflammatory cytokines and enzymes in the AGS cells are summarized in Figure 4. IL-8 mRNA expression in 20 μg/ml CAPE-treated cells was significantly suppressed as compared to *H. pylori*-stimulated control cells. Levels of TNF-α mRNA in 20 and 10 μg/ml CAPE-treated cells and IL-1β and iNOS mRNAs in all CAPE-treated cells were also markedly lower than in positive control. There were no significant differences in IL-10 and COX-2 expression among *H. pylori*-infected cells.

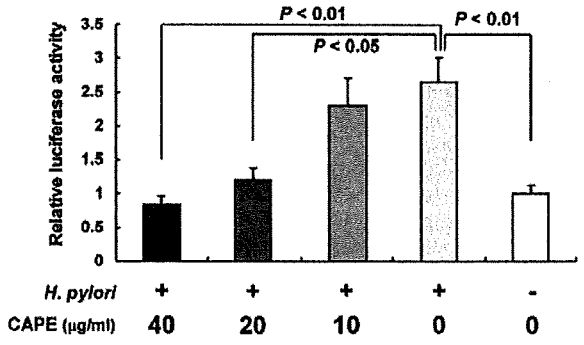

FIGURE 3 – Luciferase reporter assay for transcriptional activation of nuclear factor-κB (NF-κB) in the AGS gastric cancer cell line. Elevated transcriptional activation of NF-κB was induced after infection with *Helicobacter pylori* (*H. pylori*). Note the dose-dependent inhibition of NF-κB activation by caffeic acid phenethyl ester (CAPE) treatment compared with the vehicle control (0.1% dimethyl sulfoxide). Values are means ± SDs of data from three independent experiments.

CAPE prevents IκB-α degradation and phosphorylation of NF-κB p65 in AGS cells

We assessed the degradation of IκB-α and phosphorylation of p65 subunit by Western blot analysis (Fig. 5). Western blotting showed that *H. pylori* stimulation up-regulated the phosphorylation of p65 and IκB-α degradation in AGS cells. CAPE treatment inhibited the phosphorylation of p65 and degradation of IκB-α in a dose-dependent manner.

Average body weights, relative organ weights and serological results

Data for average body weights, titers of anti-*H. pylori* antibodies, serum gastrin levels and relative organ weights are summarized in Table II. The average body weight in the 0.1% CAPE-treated and *H. pylori*-infected group (Group A) was significantly higher than for the other *H. pylori*-infected groups (Groups B–D) ($p < 0.01$). AI values for anti-*H. pylori* antibody titers and serum gastrin levels were markedly up-regulated by *H. pylori* infection ($p < 0.01$ and $p < 0.05$, respectively). There were no significant differences in the relative organ weights of liver and kidney between 0.1% CAPE-treated and noninfected gerbils (Group E) and untreated controls (Group F). The relative kidney weights in the *H. pylori*-infected group (Group D) were markedly higher than in Group F ($p < 0.05$). No macroscopic or microscopic lesions

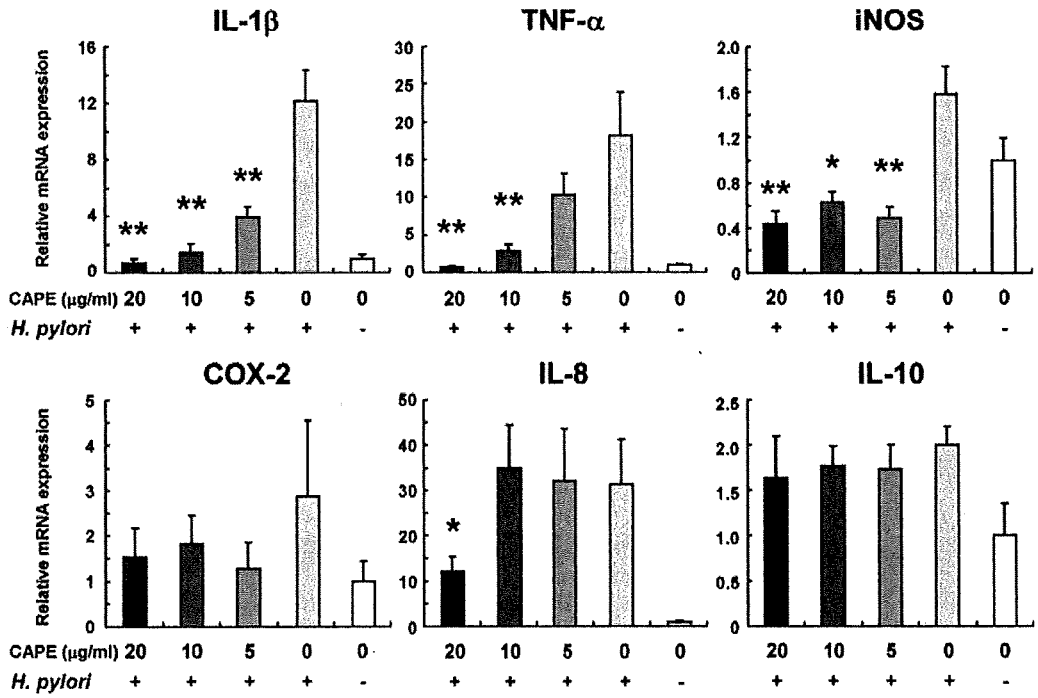

FIGURE 4 – Relative expression levels of interleukin (IL)-1β, tumor necrosis factor-α (TNF-α), inducible nitric oxide synthase (iNOS), cyclooxygenase-2 (COX-2), IL-8 and IL-10 mRNAs in the AGS gastric cancer cell line. Values were set at 1.0 in untreated control and expressed as mean ± SE relative values. Note that the *Y*-axes have different scales. *$p < 0.05$ and **$p < 0.01$ *vs. H. pylori*-infected and CAPE-untreated samples.

were observed in nonstomach internal organs, including the liver, spleen, kidney, heart and lung of all groups.

Inhibitory effects of CAPE on H. pylori*-induced gastritis*

The gastric mucosa of *H. pylori*-infected groups (Groups A–D) was generally thickened and edematous, with occasional erosions and ulceration. Such macroscopic lesions were not recognized in the stomachs of noninfected gerbils, and gastric mucosal specimens from these gerbils had normal histomorphology. Histological findings for chronic gastritis in each group are summarized in Table III. Infiltration of neutrophils in both the antrum and corpus and of mononuclear cells in the antrum of Group A animals (*H. pylori* + 0.1% CAPE) was significantly suppressed as compared to Group D ($p < 0.05$ and 0.01, respectively) (Figs. 6*a*, 6*e*, and 6*i*). There were no significant differences in scores for intestinal metaplasia, heterotopic proliferative glands and COX-2 immunoreactivity among Groups A–D. Macroscopic and microscopic analyses revealed no significant differences between gerbils in Groups E and F, so Group E was excluded from subsequent analyses of BrdU labeling indices, immunohistochemistry of NF-κB p50 and phospho-IκB-α and transcriptional expression of inflammatory factors. Immunohistochemistry of NF-κB p50 and phospho-IκB-α revealed that strong reactivity of gastric epithelium and infiltrated cells in *H. pylori*-infected gerbils, and CAPE treatment significantly reduced the immunohistochemical scores (Figs. 6*c*, 6*d*, 6*g*, 6*h*, 6*k*, and 6*l*).

BrdU labeling indices in gastric epithelial cells

In *H. pylori*-infected gerbils, BrdU-labeled epithelial nuclei were found distributed throughout the hyperplastic mucosa, while BrdU-positive cells in noninfected animals were located in the neck portions of glands (Figs. 6*b*, 6*f*, and 6*j*). At 12 weeks, BrdU labeling indices in both the antrum and corpus of Group A (*H. pylori* + 0.1% CAPE) were significantly suppressed as compared to Group D ($p < 0.01$; Fig. 7). Similarly, BrdU labeling indices in the antrum of the 0.03% CAPE-treated group (Group B) were significantly lowered ($p < 0.05$), without significant decrease in the corpus.

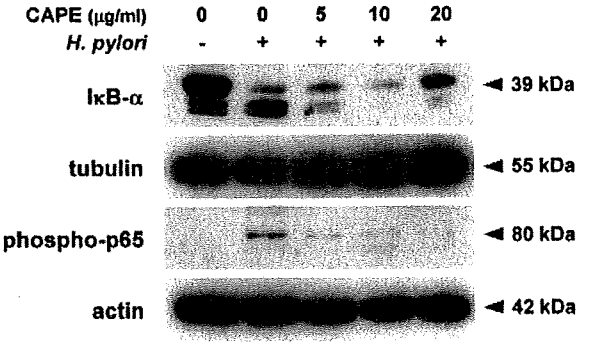

FIGURE 5 – Western blotting for IκB-α and phospho-p65 in AGS cells. CAPE prevents IκB-α degradation and p65 phosphorylation in a dose-dependent manner. A representative data of three independent experiments is shown.

Hyperplasia in isolated pyloric glands

To evaluate the effect of CAPE on *H. pylori*-induced mucosal hyperplasia, we analyzed the length of isolated glands from the pyloric mucosa (Fig. 8*a*). The average value for Group A (*H. pylori* + 0.1% CAPE) was significantly reduced compared to that for Group D ($p < 0.05$) (Fig. 8*b*).

Expression of inflammatory factors in the pyloric mucosa

RT-PCR data for mRNA expression of inflammatory cytokines and enzymes in the pyloric mucosa of gerbils are summarized in Figure 9. TNF-α and iNOS mRNA expression in Group A (*H. pylori* + 0.1% CAPE) was significantly suppressed as compared to Group D ($p < 0.05$). Levels of IL-2 mRNA in Groups A and B and IFN-γ and IL-6 mRNAs in all CAPE-treated groups (Groups A–C) were also markedly lower than in Group D ($p < 0.05$). Only very low mRNA expression was evident in Group F.

Discussion

In this study, we demonstrated that NF-κB transcriptional activation in *H. pylori*-stimulated AGS gastric cancer cells were significantly inhibited by CAPE treatment in a dose-dependent manner. This result is consistent with a previous report that CAPE inhibits *H. pylori*-induced DNA-binding activity of NF-κB in gastric cancer cells.[9] We found that CAPE treatment resulted in a decrease of the phosphorylation of NF-κB p65 subunit and inhibition of IκB-α degradation. In addition, relative quantitative real-time RT-PCR analysis revealed that mRNA expressions of several inflammatory factors including IL-1β, TNF-α, iNOS, and IL-8 in NF-κB-activated AGS cells were significantly suppressed by CAPE treatment in a dose-dependent manner, whereas there were no statistical differences in COX-2 and IL-10 expression. IκB-α degradation induces the phosphorylation of p65 and following nuclear transition of NF-κB complex. Thus, our data suggested that CAPE may prevent *H. pylori*-induced NF-κB activation and transcriptional activity of inflammatory factors through the inhibition of nuclear translocation of NF-κB.

Here we found that oral administration of CAPE effectively inhibited gastric inflammation at 0.1% in the diet with significant suppression of infiltration of neutrophils both in the antrum and corpus and mononuclear cells in the antrum at week 12. Fitzpatrick *et al.* earlier reported CAPE to inhibit TNF-α production in a rat macrophage cell line and TNF-α-stimulated IL-8 production in human colonic epithelial cells.[36] Expression of IL-8, a potent chemokine stimulus for neutrophil migration, is increased with *H. pylori* infection through NF-κB activation.[17] In this study, mRNA expression of TNF-α and IL-8 in *H. pylori*-stimulated AGS cells were significantly decreased by CAPE treatment. Similarly, CAPE markedly suppressed the expression of TNF-α and KC protein, one of the IL-8 homologues, in *H. pylori*-infected gerbils. The

TABLE II – SUMMARY OF THE ANIMAL EXPERIMENT

Group	Treatment	Effective number	Body weight (g)	Anti-*Hp* IgG titer (AI)	Serum gastrin (pg/ml)	Relative organ weights (%)	
						Liver	Kidney
A	*Hp* + 0.1% CAPE	10	81.4 ± 8.7[1]	8.4 ± 3.1[2]	187 ± 52.3[3]	3.88 ± 0.25	0.82 ± 0.07
B	*Hp* + 0.03% CAPE	10	73.5 ± 4.8	11.5 ± 4.2[2]	176 ± 35.3[3]	3.74 ± 0.17	0.82 ± 0.04
C	*Hp* + 0.01% CAPE	10	72.6 ± 4.2	15.9 ± 7.3[2]	192 ± 93.2[3]	3.66 ± 0.27	0.80 ± 0.05
D	*Hp*	10	73.0 ± 6.8	10.6 ± 5.4[2]	185 ± 45.8[3]	3.74 ± 0.13	0.83 ± 0.06[3]
E	Broth + 0.1% CAPE	5	69.5 ± 4.9	0.7 ± 0.4	126 ± 16.7	3.59 ± 0.30	0.73 ± 0.24
F	Broth	10	75.2 ± 6.4	0.5 ± 0.1	125 ± 54.8	3.75 ± 0.21	0.77 ± 0.04

Values for results are expressed as means ± SD. *Hp*, *Helicobacter pylori*; AI, arbitrary index; CAPE, caffeic acid phenethyl ester.
[1]$p < 0.01$ *vs.* Group B–D.–[2]$p < 0.01$ *vs.* Group F.–[3]$p < 0.05$ *vs.* Group F.

TABLE III – HISTOPATHOLOGICAL EVALUATION OF GASTRITIS

Group	Treatment	Effective number	Infiltration of neutrophils		Infiltration of mononuclear cells		Intestinal metaplasia		Heterotopic proliferative glands		Score of COX-2 immunohistochemistry	
			Antrum	Corpus	Antrum	Corpus	Antrum	Corpus	Antrum	Corpus	Antrum	Corpus
A	*Hp* + 0.1% CAPE	10	1.8 ± 0.4[1]	1.1 ± 0.6[1]	2.3 ± 0.3[2]	1.6 ± 0.4	0.0 ± 0.0	0.0 ± 0.0	1.1 ± 0.4	0.6 ± 0.4	1.3 ± 0.5	0.9 ± 0.7
B	*Hp* + 0.03% CAPE	10	2.6 ± 0.5	2.1 ± 0.8	2.9 ± 0.2	2.3 ± 0.5	0.1 ± 0.3	0.2 ± 0.4	1.3 ± 0.5	1.0 ± 0.7	1.6 ± 0.5	1.3 ± 0.8
C	*Hp* + 0.01% CAPE	10	2.1 ± 0.4	2.0 ± 0.9	2.6 ± 0.5	2.2 ± 0.6	0.1 ± 0.3	0.1 ± 0.3	1.1 ± 0.4	0.9 ± 0.4	1.4 ± 0.5	0.9 ± 0.6
D	*Hp*	10	2.5 ± 0.5	2.2 ± 0.7	2.9 ± 0.2	2.2 ± 0.6	0.1 ± 0.3	0.1 ± 0.3	1.1 ± 0.5	0.9 ± 0.7	1.7 ± 0.7	1.2 ± 0.8
E	Broth + 0.1% CAPE	5	0.0 ± 0.0	0.1 ± 0.2	0.0 ± 0.0	0.0 ± 0.0	0.0 ± 0.0	0.0 ± 0.0	0.0 ± 0.0	0.0 ± 0.0	0.2 ± 0.4	0.2 ± 0.4
F	Broth	10	0.1 ± 0.2	0.0 ± 0.0	0.2 ± 0.2	0.0 ± 0.0	0.0 ± 0.0	0.0 ± 0.0	0.0 ± 0.0	0.0 ± 0.0	0.1 ± 0.3	0.0 ± 0.0

Values for results are expressed as means ± SD. COX-2, cyclooxygenase-2; *Hp*, *Helicobacter pylori*; CAPE, caffeic acid phenethyl ester.
[1] $p < 0.05$ *vs.* Group D.–[2] $p < 0.01$ *vs.* Group D.

inhibitory effects of CAPE on infiltration of neutrophils observed in this study may therefore be explained by reduction of NF-κB-associated cytokines, including TNF-α and KC.

Phosphorylation of IκB-α acts as a trigger of IκB degradation, allowing the nuclear translocation of NF-κB complex and activation of gene expression. In our study, 0.1% CAPE-containing diet inhibited the immunohistochemical expression of phosphorylated IκB-α and nuclear transition of NF-κB p50 subunit in the gastric mucosa of *H. pylori*-infected gerbils, suggesting that CAPE has chemopreventive potentials by inhibiting the NF-κB pathway.

Our findings for BrdU-labeled cells in the gastric mucosa and average lengths of isolated pyloric glands suggest that *H. pylori*-induced chronic gastritis and epithelial hyper-proliferation are efficiently suppressed by CAPE administration. Previous clinical studies have demonstrated that epithelial proliferation is positively correlated with the degree of histological inflammation in the gastric mucosa of *H. pylori*-infected patients.[37] We have previously reported that the severity of gastritis plays an important role in *H. pylori*-associated gastric carcinogenesis in gerbils, with essential involvement of chronic inflammation and increased rates of cell proliferation.[38] Therefore, it is very conceivable that CAPE might reduce gastric carcinogenesis as well as chronic gastritis.

Our demonstration that mRNA expression levels of inflammatory factors including TNF-α, IFN-γ, IL-2, IL-6, iNOS and KC were significantly decreased by CAPE treatment in the pyloric mucosa of *H. pylori*-infected Mongolian gerbils is of clear interest. All these factors are known to be induced by NF-κB transcriptional activation.[5,39] It has been reported that a predominant *H. pylori*-specific Th1 response characterized by TNF-α and IFN-γ production is associated with *H. pylori*-infected gastritis.[40] Several studies have demonstrated that IFN-γ and IL-6 play important roles in progression of pyloric gastritis in *H. pylori*-infected gerbils.[20,33] In addition, TNF-α is a mediator during inflammation and tumor promotion, leading to activation of NF-κB and thereby suppression of cell death and stimulation of cell proliferation.[41] Interestingly, although significant suppressive effects of CAPE on IL-6 and IFN-γ expression in the antrum were observed in all CAPE-treated groups, gastritis was attenuated only in 0.1% CAPE-treated gerbils. Thus, our results suggest that TNF-α and iNOS might be key molecules, in addition to other factors, suppressing *H. pylori*-induced chronic gastritis in Mongolian gerbils. iNOS is also known to be up-regulated by *H. pylori* and to enhance progression of gastric inflammation and carcinogenesis through generation of reactive oxygen species.[42]

On the other hand, expression level of COX-2 was not suppressed by CAPE treatment both in *H. pylori*-stimulated AGS cells and in the pyloric mucosa of gerbils. Several studies demonstrated that gastric COX-2 expression in *H. pylori*-infected humans and rodents could be associated with repair of mucosal injury.[43–45] Thus, there is a possibility that COX-2 expression may play important roles both in mediation of gastritis and in healing of *H. pylori*-associated gastric ulceration. CAPE treatment also showed no effects on mRNA expression of IL-10 in AGS cells and the pyloric mucosa of gerbils. IL-10 has been known as an anti-inflammatory cytokine, and demonstrated to inhibit other inflammatory cytokines and chemokines in *H. pylori*-induced gastritis.[46,47] Our result of stable expression of IL-10 may reflect an increase of anti-inflammatory cytokine activity through the separate cascade from NF-κB pathway.

CAPE concentrations in the range of 0.01–0.1% were chosen for the present investigation because a previous study in mice demonstrated no toxicity at 0.15% CAPE given for 110 days.[11] In this study, there were no significant differences in relative organ weights of liver and kidney between 0.1% CAPE-treated (Group E) and nontreated gerbils (Group F). In addition, no macroscopic and microscopic lesions were observed in the non-gastric internal organs, including liver, spleen, kidney, heart and lung of CAPE-treated gerbils. Therefore, we conclude that the

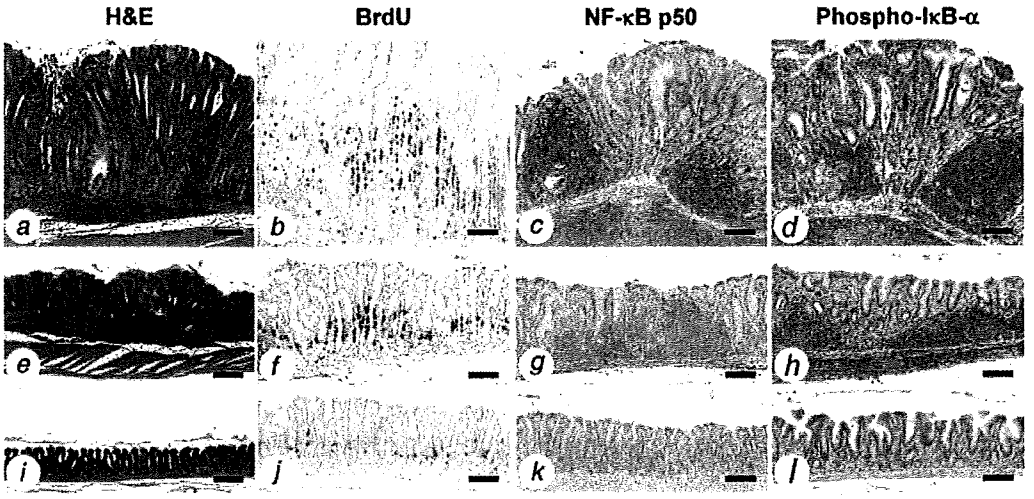

FIGURE 6 – Histopathology and immunohistochemistry findings for the gastric mucosa of Mongolian gerbils. *Helicobacter pylori* (*H. pylori*) + basal diet group (Group D, panels *a–d*), *H. pylori* + 0.1% caffeic acid phenethyl ester (CAPE) group (Group A, panels *e–h*) and Broth + basal diet group (Group F, panels *i–l*). (*a*) Marked mucosal hyperplasia with severe infiltration of neutrophils and mononuclear cells (H&E, ×50, Bar = 200 μm). (*b*) Large numbers of BrdU-positive cells are apparent in hyperplastic mucosal epithelium (BrdU immunostaining, ×100, Bar = 100 μm). (*c* and *d*) Strong expression of NF-κB p50 and phospho-IκB-α is observed in gastric epithelium and infiltrated cells (NF-κB p50 and phospho-IκB-α immunostaining, respectively, ×100, Bar = 100 μm). (*e*) Mild to moderate gastritis (H&E, ×50, Bar = 200 μm). (*f*) Note moderate numbers of BrdU-positive cells (BrdU, ×100, Bar = 100 μm). (*g* and *h*) Relatively weak expression of NF-κB p50 and phospho-IκB-α in 0.1% CAPE-treated gerbils (NF-κB p50 and phospho-IκB-α, ×100, Bar = 100 μm). (*i*) No lesions are observed in the gastric mucosa of a noninfected gerbil (H&E, ×50, Bar = 200 μm). (*j*) BrdU-positive cells are present only in the proliferative zone of a noninfected animal (BrdU, ×100, Bar = 100 μm). (*k* and *l*) NF-κB p50 and phospho-IκB-α expression is weak in a noninfected gerbil (NF-κB p50 and phospho-IκB-α, ×100, Bar = 100 μm).

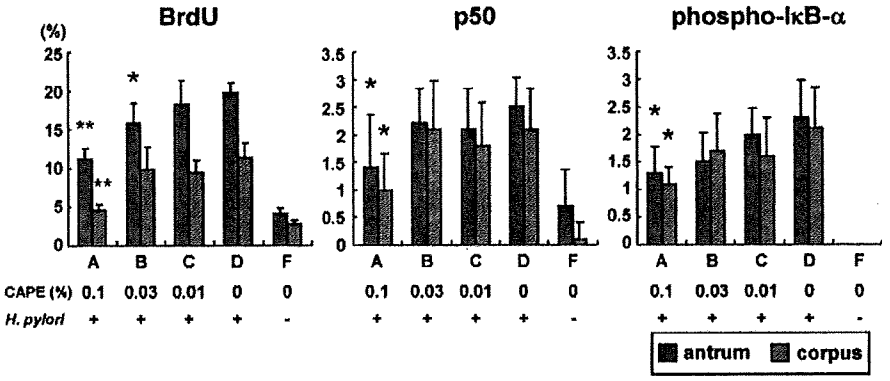

FIGURE 7 – Immunohistochemical analysis of BrdU, NF-κB p50, and phospho-IκB-α staining in the antrum and corpus of Mongolian gerbils. BrdU staining was evaluated by mean percentages of BrdU-positive cells among total cells in 10 selected glands, and NF-κB p50 and phospho-IκB-α staining were scored 0–4. Data are presented as mean ± SD values. $*p < 0.05$ and $**p < 0.01$ *vs.* Group D.

toxicity of CAPE is negligible at the doses used in the present study. Our data showed that relative kidney weight of *H. pylori*-infected group (Group D) was statistically higher than that of Group F. Several authors have discussed whether *H. pylori* infection is associated with the pathogenesis of renal failures in humans, but the relationship is still unclear.[48,49] Because there were no macroscopic and microscopic renal lesions in the gerbils, more detail examination is needed to clarify the association of renal weight change and *H. pylori* infection. Regarding body weight, 0.1% CAPE-treated and *H. pylori*-infected gerbils (Group A) were heavier than those in other infected groups (Groups B–D). However, animals in Group E showed no significant increase. Since there were no marked differences in serum total cholesterol and triglyceride levels between Groups A and D (data not shown), there may not be significant relevance between CAPE ingestion and body weight change.

In conclusion, our study clearly demonstrated: (1) CAPE treatment inhibits *H. pylori*-induced NF-κB activation by suppression of IκB-α degradation and phosphorylation of p65 in a gastric cancer cell line, and (2) CAPE exerts anti-inflammatory effects on *H. pylori*-induced gastritis in Mongolian gerbils with reduction of nuclear transition of NF-κB p50 through phosphorylation of IκB-α

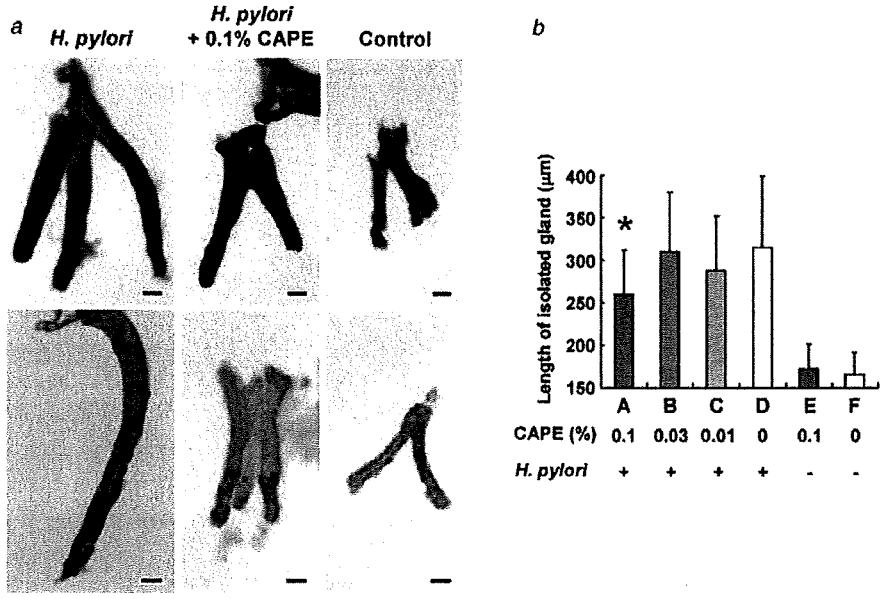

FIGURE 8 – Isolated glands from the pyloric mucosa of Mongolian gerbils. (*a*) Histopathology and immunohistochemistry of isolated pyloric glands (Upper column, H&E; Lower column, BrdU staining, ×200, Bar = 25 μm). Note the *Helicobacter pylori*-induced hyperplasia and cell proliferation activity is attenuated by 0.1% CAPE treatment. (*b*) Average lengths of isolated pyloric glands of Mongolian gerbils. Data are mean ± SD values. Note that the *Y*-axis starts from 150. **p* < 0.05 *vs.* Group D.

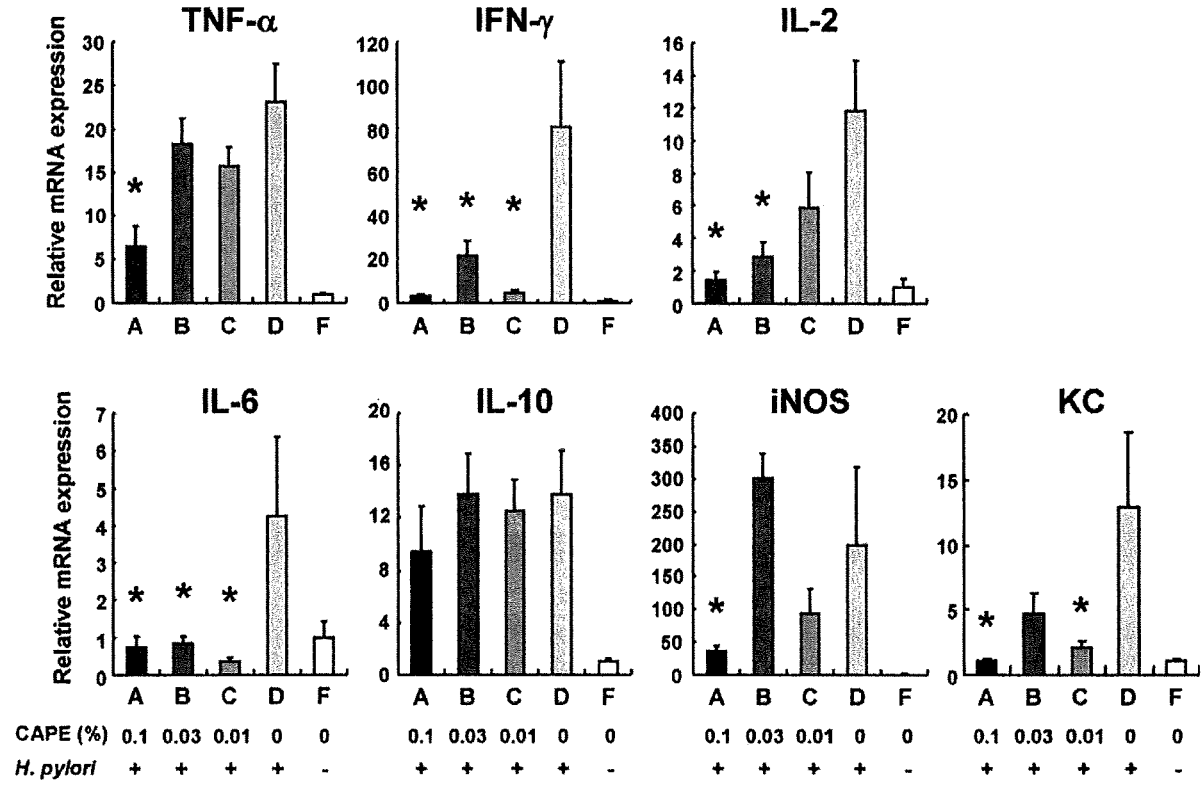

FIGURE 9 – Relative expression levels of tumor necrosis factor-α (TNF-α), interferon-γ (IFN-γ), interleukin (IL)-2, IL-6, IL-10, inducible nitric oxide synthase (iNOS), and KC mRNAs in the pyloric mucosa of Mongolian gerbils at 12 weeks postinfection. Values were set at 1.0 in Group F and expressed as mean ± SE relative values. Note that the *Y*-axes have different scales. **p* < 0.05 *vs.* Group D.

and suppression of the mRNA expression of many NF-κB-associated inflammatory factors. These results suggest that CAPE may have potential as an alternative drug for chemoprevention of chronic active gastritis and other *H. pylori*-associated gastric disorders, including stomach adenocarcinomas.

Acknowledgements

The authors thank Ms. Noriko Saito and Ms. Ayumi Saito for their expert technical assistance.

References

1. Bonizzi G, Karin M. The two NF-κB activation pathways and their role in innate and adaptive immunity. Trends Immunol. 2004;25:280–8.
2. Coussens LM, Werb Z. Inflammation and cancer. Nature 2002;420:860–7.
3. Calzado MA, Bacher S, Schmitz ML. NF-κB inhibitors for the treatment of inflammatory diseases and cancer. Curr Med Chem 2007; 14:367–76.
4. Inoue J, Gohda J, Akiyama T, Semba K. NF-κB activation in development and progression of cancer. Cancer Sci 2007;98:268–74.
5. Umezawa K, Ariga A, Matsumoto N. Naturally occurring and synthetic inhibitors of NF-κB functions. Anticancer Drug Des 2000; 15:239–44.
6. Olivier S, Robe P, Bours V. Can NF-κB be a target for novel and efficient anti-cancer agents? Biochem Pharmacol 2006;72: 1054–68.
7. Natarajan K, Singh S, Burke TR, Jr, Grunberger D, Aggarwal BB. Caffeic acid phenethyl ester is a potent and specific inhibitor of activation of nuclear transcription factor NF-κB. Proc Natl Acad Sci USA 1996;93:9090–5.
8. Grunberger D, Banerjee R, Eisinger K, Oltz EM, Efros L, Caldwell M, Estevez V, Nakanishi K. Preferential cytotoxicity on tumor cells by caffeic acid phenethyl ester isolated from propolis. Experientia 1988;44:230–2.
9. Abdel-Latif MM, Windle HJ, Homasany BS, Sabra K, Kelleher D. Caffeic acid phenethyl ester modulates *Helicobacter pylori*-induced nuclear factor-kappa B and activator protein-1 expression in gastric epithelial cells. Br J Pharmacol 2005;146:1139–47.
10. Chen MF, Keng PC, Lin PY, Yang CT, Liao SK, Chen WC. Caffeic acid phenethyl ester decreases acute pneumonitis after irradiation *in vitro* and *in vivo*. BMC Cancer 2005;5:158–66.
11. Mahmoud NN, Carothers AM, Grunberger D, Bilinski RT, Churchill MR, Martucci C, Newmark HL, Bertagnolli MM. Plant phenolics decrease intestinal tumors in an animal model of familial adenomatous polyposis. Carcinogenesis 2000;21:921–7.
12. Carrasco-Legleu CE, Marquez-Rosado L, Fattel-Fazenda S, Arce-Popoca E, Perez-Carreon JI, Villa-Trevino S. Chemoprotective effect of caffeic acid phenethyl ester on promotion in a medium-term rat hepatocarcinogenesis assay. Int J Cancer 2004;108:488–92.
13. Uemura N, Okamoto S, Yamamoto S, Matsumura N, Yamaguchi S, Yamakido M, Taniyama K, Sasaki N, Schlemper RJ. *Helicobacter pylori* infection and the development of gastric cancer. N Engl J Med 2001;345:784–9.
14. IARC Working Group on the Evaluation of Carcinogenic Risks to Humans. Infection with *Helicobacter pylori*. In: Schistosomes, Liver Flukes and *Helicobacter pylori*. IARC Monographs on the Evaluation of Carcinogenic Risks to Humans, vol.61. Lyon, World Health Organization/International Agency for Research on Cancer, 1994.177–241.
15. Malfertheiner P, Megraud F, O'Morain C, Bazzoli F, El-Omar E, Graham D, Hunt R, Rokkas T, Vakil N, Kuipers EJ. Current concepts in the management of *Helicobacter pylori* infection: the Maastricht III Consensus Report. Gut 2007;56:772–81.
16. Gerrits MM, van Vliet AH, Kuipers EJ, Kusters JG. *Helicobacter pylori* and antimicrobial resistance: molecular mechanisms and clinical implications. Lancet Infect Dis 2006;6:699–709.
17. Keates S, Hitti YS, Upton M, Kelly CP. *Helicobacter pylori* infection activates. NF-κB in gastric epithelial cells. Gastroenterology 1997; 113:1099–109.
18. Maeda S, Yoshida H, Ogura K, Mitsuno Y, Hirata Y, Yamaji Y, Akanuma M, Shiratori Y, Omata M. *H. pylori* activates NF-κB through a signaling pathway involving IκB kinases. NF-κB-inducing kinase. TRAF2, and TRAF6 in gastric cancer cells. Gastroenterology 2000; 119:97–108.
19. Crabtree JE, Court M, Aboshkiwa MA, Jeremy AH, Dixon MF, Robinson PA. Gastric mucosal cytokine and epithelial cell responses to *Helicobacter pylori* infection in Mongolian gerbils. J Pathol 2004; 202:197–207.
20. Yamaoka Y, Yamauchi K, Ota H, Sugiyama A, Ishizone S, Graham DY, Maruta F, Murakami M, Katsuyama T. Natural history of gastric mucosal cytokine expression in *Helicobacter pylori* gastritis in Mongolian gerbils. Infect Immun 2005;73:2205–12.
21. Kim SG, Kim JS, Kim JM, Chae Jung H, Sung Song I. Inhibition of proinflammatory cytokine expression by NF-κB (p65) antisense oligonucleotide in *Helicobacter pylori*-infected mice. Helicobacter 2005; 10:559–66.
22. Ogura K, Maeda S, Nakao M, Watanabe T, Tada M, Kyutoku T, Yoshida H, Shiratori Y, Omata M. Virulence factors of *Helicobacter pylori* responsible for gastric diseases in Mongolian gerbil. J Exp Med 2000;192:1601–10.
23. Wu CS, Chen MF, Lee IL, Tung SY. Predictive role of nuclear factor-κB activity in gastric cancer: a promising adjuvant approach with caffeic acid phenethyl ester. J Clin Gastroenterol 2007;41:894–900.
24. Tatematsu M, Tsukamoto T, Inada K. Stem cells and gastric cancer: role of gastric and intestinal mixed intestinal metaplasia. Cancer Sci 2003;94:135–41.
25. Otsuka T, Tsukamoto T, Tanaka H, Inada K, Utsunomiya H, Mizoshita T, Kumagai T, Katsuyama T, Miki K, Tatematsu M. Suppressive effects of fruit-juice concentrate of *Prunus mume* Sieb. et Zucc. (Japanese apricot. Ume) on *Helicobacter pylori*-induced glandular stomach lesions in Mongolian gerbils. Asian Pac J Cancer Prev 2005;6:337–41.
26. Toyoda T, Tsukamoto T, Mizoshita T, Nishibe S, Deyama T, Takenaka Y, Hirano N, Tanaka H, Takasu S, Ban H, Kumagai T, Inada K, et al. Inhibitory effect of nordihydroguaiaretic acid, a plant lignan, on *Helicobacter pylori*-associated gastric carcinogenesis in Mongolian gerbils. Cancer Sci 2007;98:1689–95.
27. Cao X, Tsukamoto T, Seki T, Tanaka H, Morimura S, Cao L, Mizoshita T, Ban H, Toyoda T, Maeda H, Tatematsu M. 4-Vinyl-2,6-dimethoxyphenol (canolol) suppresses oxidative stress and gastric carcinogenesis in *Helicobacter pylori*-infected carcinogen-treated Mongolian gerbils. Int J Cancer 2008;122:1445–54.
28. Shimizu N, Inada KI, Tsukamoto T, Nakanishi H, Ikehara Y, Yoshikawa A, Kaminishi M, Kuramoto S, Tatematsu M. New animal model of glandular stomach carcinogenesis in Mongolian gerbils infected with *Helicobacter pylori* and treated with a chemical carcinogen. J Gastroenterol 1999;34(Suppl 11):61–6.
29. Tsukamoto T, Fukami H, Yamanaka S, Yamaguchi A, Nakanishi H, Sakai H, Aoki I, Tatematsu M. Hexosaminidase-altered aberrant crypts, carrying decreased hexosaminidase alpha and beta subunit mRNAs, in colon of 1,2-dimethylhydrazine-treated rats. Jpn J Cancer Res 2001;92:109–18.
30. Dixon MF, Genta RM, Yardley JH, Correa P. Classification and grading of gastritis. The updated Sydney System. International Workshop on the Histopathology of Gastritis, Houston 1994. Am J Surg Pathol 1996;20:1161–81.
31. Ikeno T, Ota H, Sugiyama A, Ishida K, Katsuyama T, Genta RM, Kawasaki S. *Helicobacter pylori*-induced chronic active gastritis, intestinal metaplasia, and gastric ulcer in Mongolian gerbils. Am J Pathol 1999;154:951–60.
32. Tanaka T, Kohno H, Suzuki R, Hata K, Sugie S, Niho N, Sakano K, Takahashi M, Wakabayashi K. Dextran sodium sulfate strongly promotes colorectal carcinogenesis in Apc(Min/+) mice: inflammatory stimuli by dextran sodium sulfate results in development of multiple colonic neoplasms. Int J Cancer 2006;118:25–34.
33. Kudo T, Lu H, Wu JY, Ohno T, Wu MJ, Genta RM, Graham DY, Yamaoka Y. Pattern of transcription factor activation in *Helicobacter pylori*-infected Mongolian gerbils. Gastroenterology 2007;132:1024–38.
34. Kim M, Miyamoto S, Yasui Y, Oyama T, Murakami A, Tanaka T. Zerumbone, a tropical ginger sesquiterpene, inhibits colon and lung carcinogenesis in mice. Int J Cancer 2009;124:264–71.
35. Tsukamoto T, Inada K, Tanaka H, Mizoshita T, Mihara M, Ushijima T, Yamamura Y, Nakamura S, Tatematsu M. Down-regulation of a gastric transcription factor. Sox2, and ectopic expression of intestinal homeobox genes Cdx1 and Cdx2: inverse correlation during progression from gastric/intestinal-mixed to complete intestinal metaplasia. J Cancer Res Clin Oncol 2004;130:135–45.
36. Fitzpatrick LR, Wang J, Le T. Caffeic acid phenethyl ester, an inhibitor of nuclear factor-κB, attenuates bacterial peptidoglycan polysaccharide-induced colitis in rats. J Pharmacol Exp Ther 2001;299:915–20.
37. Naumann M, Crabtree JE. *Helicobacter pylori*-induced epithelial cell signalling in gastric carcinogenesis. Trends Microbiol 2004;12:29–36.
38. Cao X, Tsukamoto T, Nozaki K, Tanaka H, Cao L, Toyoda T, Takasu S, Ban H, Kumagai T, Tatematsu M. Severity of gastritis determines glandular stomach carcinogenesis in *Helicobacter pylori*-infected Mongolian gerbils. Cancer Sci 2007;98:478–83.
39. Naito Y, Yoshikawa T. Molecular and cellular mechanisms involved in *Helicobacter pylori*-induced inflammation and oxidative stress. Free Radic Biol Med 2002;33:323–36.

40. D'Elios MM, Manghetti M, De Carli M, Costa F, Baldari CT, Burroni D, Telford JL, Romagnani S, Del Prete G. T helper 1 effector cells specific for *Helicobacter pylori* in the gastric antrum of patients with peptic ulcer disease. J Immunol 1997;158:962–7.
41. Karin M, Greten FR. NF-κB: linking inflammation and immunity to cancer development and progression. Nat Rev Immunol 2005;5:749–59.
42. Rajnakova A, Moochhala S, Goh PM, Ngoi S. Expression of nitric oxide synthase, cyclooxygenase, and p53 in different stages of human gastric cancer. Cancer Lett 2001;172:177–85.
43. Jackson LM, Wu KC, Mahida YR, Jenkins D, Hawkey CJ. Cyclooxygenase (COX) 1 and 2 in normal, inflamed, and ulcerated human gastric mucosa. Gut 2000;47:762–70.
44. Toyoda T, Tsukamoto T, Hirano N, Mizoshita T, Kato S, Takasu S, Ban H, Tatematsu M. Synergistic upregulation of inducible nitric oxide synthase and cyclooxygenase-2 in gastric mucosa of Mongolian gerbils by a high-salt diet and *Helicobacter pylori* infection. Histol Histopathol 2008;23:593–9.
45. Mizuno H, Sakamoto C, Matsuda K, Wada K, Uchida T, Noguchi H, Akamatsu T, Kasuga M. Induction of cyclooxygenase 2 in gastric mucosal lesions and its inhibition by the specific antagonist delays healing in mice. Gastroenterology 1997;112: 387–97.
46. Crabtree JE. Role of cytokines in pathogenesis of *Helicobacter pylori*-induced mucosal damage. Dig Dis Sci 1998;43:46S–55S.
47. Bodger K, Wyatt JI, Heatley RV. Gastric mucosal secretion of interleukin-10: relations to histopathology. *Helicobacter pylori* status, and tumour necrosis factor-alpha secretion. Gut 1997;40:739–44.
48. Nagashima R, Maeda K, Yuda F, Kudo K, Saitoh M, Takahashi T. *Helicobacter pylori* antigen in the glomeruli of patients with membranous nephropathy. Virchows. Arch 1997;431:235–9.
49. Sugimoto M, Sakai K, Kita M, Imanishi J, Yamaoka Y. Prevalence of *Helicobacter pylori* infection in long-term hemodialysis patients. Kidney Int 2009;75:96–103.

Pitavastatin Fails to Lower Serum Lipid Levels or Inhibit Gastric Carcinogenesis in *Helicobacter pylori*–Infected Rodent Models

Takeshi Toyoda,[1] Tetsuya Tsukamoto,[1] Shinji Takasu,[1] Naoki Hirano,[1] Hisayo Ban,[1] Liang Shi,[1] Toshiko Kumagai,[3] Takuji Tanaka[4] and Masae Tatematsu[1,2]

Abstract Statins are commonly used lipid-lowering drugs that reduce the risk of cardiovascular morbidity and mortality. Although recent studies have pointed to chemopreventive effects of statins against various cancers, their efficacy for gastric cancer is unclear. Here, we examined the effects of pitavastatin, a lipophilic statin, on *Helicobacter pylori* (*H. pylori*)–associated stomach carcinogenesis and gastritis using Mongolian gerbil and mouse models. The animals were allocated to *H. pylori* + *N*-methyl-*N*-nitrosourea administration (gerbils, 52 weeks) or *H. pylori* infection alone groups (gerbils and mice, 12 weeks). After *H. pylori* infection, they were fed basal diets containing 0 to 10 ppm of pitavastatin. The incidences of *H. pylori*–associated gastric adenocarcinomas and degrees of chronic gastritis were not decreased by pitavastatin compared with those of control values. Expression of interleukin-1β and tumor necrosis factor-α mRNAs in the pyloric mucosa was markedly up-regulated in pitavastatin-treated animals. Furthermore, in the *H. pylori*–infected groups, serum total cholesterol, triglyceride, and low-density lipoprotein levels were significantly increased by pitavastatin treatment, contrary to expectation. In the short-term study, *H. pylori*–infected gerbils and mice also showed significant up-regulation of serum triglyceride levels by pitavastatin, whereas total cholesterol was markedly reduced and low-density lipoprotein exhibited a tendency for decrease in noninfected animals. These findings indicate pitavastatin to be ineffective for suppressing gastritis and chemoprevention of gastric carcinogenesis in *H. pylori*–infected gerbils. Our serologic results also suggest that the *H. pylori* infection and consequent severe chronic gastritis interfere with the cholesterol-lowering effects of pitavastatin.

Statins are widely used drugs for the treatment of hypercholesterolemia, with beneficial effects on cardiovascular disease (1, 2). They are potent inhibitors of 3-hydroxy-3-methylglutaryl CoA reductase, a rate-limiting enzyme in cholesterol biosynthesis, and decrease serum lipid levels, especially low-density lipoprotein (LDL) cholesterol and triglyceride (TG). Recent studies have shown multifunctionality of statins, including anti-inflammatory and antiangiogenic effects, independent of their lipid-lowering influence (3, 4). Epidemiologic research has also suggested chemopreventive properties for various types of cancer, including colorectal tumors (5–7). However, studies of cancer prevention by statins have produced conflicting results (8–12).

Stomach cancer is the fourth most common cancer and second leading cause of cancer-related death worldwide (13). In spite of its importance, no large epidemiologic research into inhibitory effects of statin on stomach carcinogenesis has thus far been conducted. Moreover, there has been no *in vivo* examination of gastric carcinogenesis using animal models, although several rodent studies have shown statins to be preventive agents for colorectal cancer (14, 15). *Helicobacter pylori* (*H. pylori*) is now recognized as a major risk factor for chronic active gastritis and stomach cancer development (16, 17). In addition, it has been suggested to be also associated with coronary heart disease due to the alteration of the serum lipid profile (18, 19). Therefore, there is a possibility that *H. pylori* infection might influence the pharmacologic activity of statins.

The Mongolian gerbil (*Meriones unguiculatus*) provides a useful animal model of *H. pylori*–induced chronic active gastritis, allowing investigation of morbidity-related pathologic epithelial alterations in gastric mucosa and their development into gastric neoplasia (20). The purpose of the present study

Authors' Affiliations: [1]Division of Oncological Pathology, Aichi Cancer Center Research Institute; [2]Division of Cancer Genetics, Nagoya University Graduate School of Medicine, Nagoya, Japan; [3]Central Clinical Laboratories, Shinshu University Hospital, Matsumoto, Japan; and [4]1st Department of Pathology, Kanazawa Medical University, Ishikawa, Japan

Received 2/17/09; revised 4/20/09; accepted 5/11/09; published OnlineFirst 7/21/09.

Grant support: Grant-in-Aid for the Third-term Comprehensive 10-year Strategy for Cancer Control; Grant-in-Aid for Cancer Research from the Ministry of Health, Labour and Welfare, Japan; and Grant-in-Aid from the Ministry of Education, Culture, Sports, Science and Technology, Japan.

Requests for reprints: Tetsuya Tsukamoto, Division of Oncological Pathology, Aichi Cancer Center Research Institute, 1-1 Kanokoden, Chikusa-ku, Nagoya 464-8681, Japan. Phone: 81-52-762-6111; Fax: 81-52-764-2972; E-mail: ttsukamt@aichi-cc.jp.

doi:10.1158/1940-6207.CAPR-09-0082

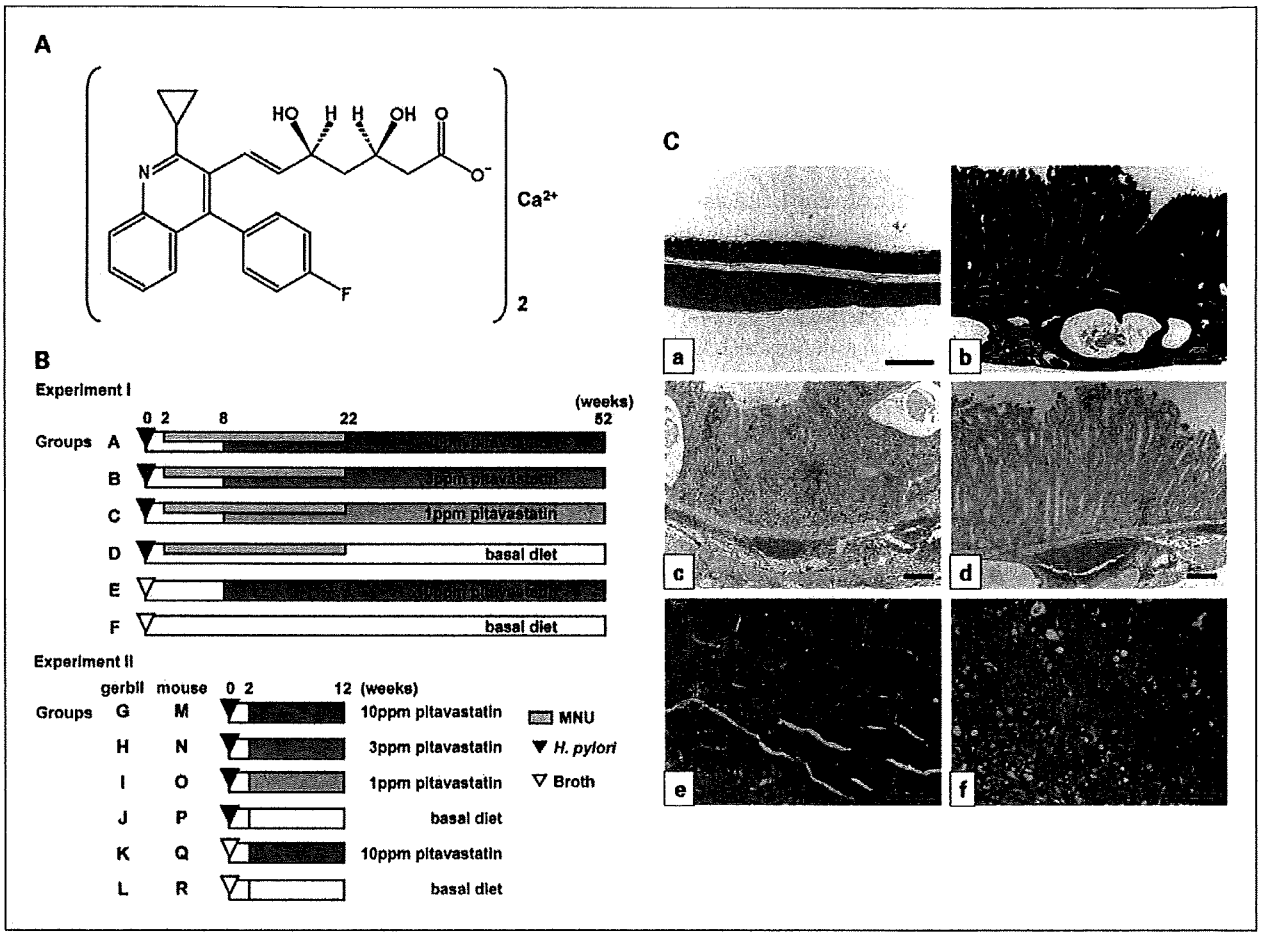

Fig. 1. *A*, chemical structure of pitavastatin. $C_{50}H_{46}CaF_2N_2O_8$ (molecular weight, 880.98). *B*, experimental design. Six-week-old male Mongolian gerbils or C57BL/6J mice were inoculated with *H. pylori* (ATCC43504 strain for gerbils or SS1 strain for mice) or Brucella broth. In the long-term experiment (experiment I), the gerbils (groups A-F) were given 10 ppm MNU in their drinking water for 20 wk and basal diet (CE-2) containing pitavastatin (0, 1, 3, or 10 ppm) from weeks 8 to 52. In the short-term experiment (experiment II), the gerbils (groups G-L) and mice (groups M-R) were given CE-2 diet containing pitavastatin from weeks 2 to 12. *C*, histopathology and immunohistochemistry in experiment I. a, normal gastric mucosa in a group F (untreated control group) gerbil at 52 wk (H&E). Magnification, ×30. *Bar*, 500 μm. b, marked infiltration of inflammatory cells and hyperplasia is evident in a group D (*H. pylori* + MNU) gerbil at 52 wk after infection (H&E). Magnification, ×30. *Bar*, 500 μm. c and d, note that the intensity of iNOS immunoreactivity in a group A (*H. pylori* + MNU + 10 ppm pitavastatin) gerbil is higher than that in a group D gerbil. Magnification, ×50 (*c* and *d*). *Bar*, 200 μm. e, well-differentiated adenocarcinoma in the glandular stomach of a group D gerbil (H&E). Magnification, ×160. *Bar*, 100 μm. f, poorly differentiated adenocarcinoma at 52 wk in a group D gerbil (H&E). Magnification, ×200. *Bar*, 100 μm.

was to evaluate the effect of pitavastatin, a recently developed lipophilic statin (21), on *H. pylori*–associated gastric carcinogenesis, and to clarify the effect of *H. pylori* infection and associated chronic gastritis on cholesterol-lowering effects of pitavastatin, using two rodent models.

Materials and Methods

Chemicals and diets

Pitavastatin (Fig. 1A) was kindly donated by Kowa Pharmaceutical Co. Ltd. CE-2 powder diet was purchased from Clea Japan, Inc. Experimental diets containing pitavastatin were prepared every 8 d in our laboratory and stored in a refrigerator. Food cups were replenished with fresh diet every second day. The gastric carcinogen *N*-methyl-*N*-nitrosourea (MNU) was purchased from Sigma Chemical, dissolved in distilled water at the concentration of 10 ppm, and administered via light-shielded bottles in drinking water *ad libitum*. MNU solutions were freshly prepared thrice per week.

Inoculation of *H. pylori*

H. pylori was prepared by the same method as described previously (22). Briefly, *H. pylori* strain ATCC43504 or Sydney strain 1 (American Type Culture Collection) was grown in Brucella broth (Becton Dickinson), containing 7% (v/v) heat-inactivated fetal bovine serum, at 37°C under microaerophilic conditions using an Anaero Pack Campylo (Mitsubishi Gas Chemical Co., Inc.) at high humidity for 24 h. After 24-h fasting, animals were inoculated via an oral catheter with 1.0 mL (gerbils) or 0.8 mL (mice) of aliquots of *H. pylori* culture containing 1.0×10^8 colony-forming units/mL of the organisms. Before inoculation, the broth cultures of *H. pylori* were checked under a phase-contrast microscope (TMS; Nikon Co.) for bacterial shape and mobility. Four hours later, the animals were again allowed free access to food.

Animals and experimental protocol

Two hundred thirty-three specific pathogen-free male Mongolian gerbils (MGS/Sea; Kyudo Co. Ltd.) and 118 specific pathogen-free male C57BL/6J mice (Clea Japan), 6 wk old, were used in this study.

All animals were housed in plastic cages on hardwood chip bedding in an air-conditioned biohazard room with a 12-h light/12-h dark cycle and allowed free access to food and water. The experimental designs were approved by the Animal Care Committee of the Aichi Cancer Center Research Institute, and the animals were cared for in accordance with institutional guidelines as well as the Guidelines for Proper Conduct of Animal Experiments (Science Council of Japan, June 1, 2006). The experimental design is illustrated in Fig. 1B. The animals were allocated to experiments I and II.

In experiment I, 175 gerbils were divided into six groups (groups A-F). Two weeks after inoculation of *H. pylori*, gerbils of groups A to D were administered MNU for 20 wk, and groups E and F were given broth and autoclaved distilled water. From weeks 8 to 52, the gerbils received CE-2 diets containing pitavastatin at concentrations of 10 (groups A and E), 3 (group B), 1 (group C), or 0 ppm (groups D and F). All surviving animals were sacrificed under deep anesthesia at 52 wk after inoculation and subjected to laparotomy with excision of the stomach.

In experiment II, a total of 58 gerbils and 118 mice were divided into six groups (groups G-L and M-R, respectively). Groups G to J and M to P were inoculated with *H. pylori* as in experiment I. From weeks 2 to 12, the animals received CE-2 diet containing pitavastatin at the concentrations of 10 (groups G, K, M, and Q), 3 (groups H and N), 1 (groups I and O), or 0 ppm (groups J, L, P, and R). Sacrifice was at 12 wk after inoculation.

Histology and immunohistochemistry

For histologic and immunohistochemical examination, the stomachs were fixed in 10% neutral-buffered formalin for 24 h, sliced along the longitudinal axis into strips of equal width, and embedded in paraffin. Serial sections (4 μm thick) were prepared and stained with H&E for morphologic observation and immunohistochemistry for cyclooxygenase-2 (COX-2) and inducible nitric oxide synthase (iNOS). The degree of chronic active gastritis was graded according to criteria modified from the updated Sydney System (23), by scoring the infiltration of neutrophils and mononuclear cells, as well as intestinal metaplasia and heterotopic proliferative glands (HPGs), on a four-point scale (0-3; 0, normal; 1, mild; 2, moderate; 3, marked). Immunohistochemical analysis of COX-2 and iNOS was carried out with a mouse monoclonal anti-COX-2 antibody (diluted 1:200; BD Biosciences) and a rabbit polyclonal anti-iNOS antibody (1:500; Calbiochem) as previously described (24). To quantitate the degree of staining, the grading system used the following criteria: grade 0 (negative), grades 1 to 3 (increasing degrees of intermediate immunoreactivity), and grade 4 (extensive reactivity; ref. 25). The sections were analyzed on BX50 light microscope (Olympus). Images were captured using AxioVision 4.6 software (Carl Zeiss Co. Ltd.) and further processed with Adobe Photoshop software (Adobe Systems).

Serologic examination

Before removal of the stomachs, blood samples were collected from the inferior vena cava after laparotomy. Sera were separated from blood and the total cholesterol (T-Chol), TG, high-density lipoprotein (HDL), and LDL levels were measured by ELISA (SRL, Inc.). The titers of anti–*H. pylori* antibodies were also determined with an ELISA kit (Biomerica) and values were expressed using an arbitrary index (26).

Analysis of mRNA expression of inflammatory factors by real-time quantitative PCR

Total RNA was extracted from the antrum and corpus in the glandular stomach of gerbils using a QuickGene RNA Tissue Kit SII (Fujifilm). After DNase treatment, first-strand cDNAs were synthesized using a SuperScript III First-Strand Synthesis System for reverse transcription-PCR (Invitrogen) according to the manufacturer's instructions. Quantitative PCR of interleukin (IL)-1β, tumor necrosis factor (TNF)-α, and iNOS was done using a StepOne Real-Time PCR System (Applied Biosystems) with the gerbil-specific *glyceraldehyde-3-phosphate dehydrogenase* gene as an internal control. The PCR was done basically following the manufacturer's instructions using a QuantiTect SYBR Green PCR kit (Qiagen). For PCR amplification, the following primers were used: glyceraldehyde-3-phosphate dehydrogenase, 5′-AACGGCACAGTCAAGGCTGAGAACG-3′ and 5′-CAACATACTCGGCACCGGCATCG-3′; IL-1β, 5′-TTGGGCCTCAAGGGAAAGAATCTGT-3′ and 5′-GGTATTGTTTGGGGTCCACGCTCTC-3′; TNF-α, 5′-GCCCCCACCTCGTGCTCCTCAC-3′ and 5′-GGCAGGGGCTCTTGATGGCAGACAG-3′; and iNOS, 5′-GCTTGAGCGAGGAGCAGGTTGAGGA-3′ and 5′-CGCTGGCCTTTTTCACCCCATAGGA-3′. Specificity of the PCR was confirmed using a melt curve program provided with the StepOne software. To further confirm that there was no obvious primer dimer formation or amplification of any extra bands, the samples were electrophoresed in 3% agarose gels and visualized with ethidium bromide after the StepOne reaction. Relative quantification was done as previously established using the internal control without the necessity for external standards (27). The expression levels of mRNAs were expressed relative to 1.0 in the control group.

Table 1. Summary of the general data and incidences of gastric carcinomas in Mongolian gerbils in experiment I

Group (*n*)	Treatment	BW (g)	Anti-Hp IgG titer (AI)	Relative organ weights (%)		Adenocarcinoma		
				Liver	Kidney	Well	Por	Incidence (%)
A (40)	Hp + MNU + 10 ppm PS	96.6 ± 14.9	257.8 ± 225.4	5.09 ± 0.81*	0.85 ± 0.06	15	3	18/40 (45.0)
B (39)	Hp + MNU + 3 ppm PS	97.3 ± 9.4	415.4 ± 452.3	5.08 ± 0.77*	0.84 ± 0.07	22	0	22/39 (56.4)
C (40)	Hp + MNU + 1 ppm PS	89.1 ± 16.6	233.6 ± 218.3	4.76 ± 1.00*	0.85 ± 0.07	19	1	20/40 (50.0)
D (41)	Hp + MNU	91.5 ± 14.9	296.5 ± 197.7	4.73 ± 1.03*	0.85 ± 0.11	15	2	17/41 (41.5)
E (10)	Broth + 10 ppm PS	94.7 ± 9.7	3.8 ± 3.2	3.84 ± 0.11	0.71 ± 0.06*	0	0	0/10 (0)
F (5)	Untreated control	89.7 ± 12.9	ND	3.65 ± 0.31	0.83 ± 0.07	0	0	0/5 (0)

NOTE: Values for results are expressed as mean ± SD.

Abbreviations: BW, body weight; Hp, *Helicobacter pylori*; AI, arbitrary index; Well, well-differentiated adenocarcinoma; Por, poorly differentiated adenocarcinoma; PS, pitavastatin; ND, not done.

*$P < 0.01$ versus group F.